Experimental Probes and Techniques

Reading: Kolasinski, ch.2

The techniques of surface science

- AES, AFM, EELS, ESCA, EXAFS, FEM, FIM, FTIR, HEIS, HPXPS, HREELS, IRAS, ISS, LEED, LEIS, NEXAFS, NMR, RBS, SERS, SEXAFS, SFG, SHG, SIMS, STM, TEM, TDS, UPS, XANES, SPS, XRD…

- Surface properties: structure, composition, oxidation states, chemical properties, electronic properties, mechanical properties → atomic resolution, smaller energy resolution, shorter time scales, in situ, high pressure

- Sources: electrons, atoms, ions, photons

Ultrahigh vacuum (UHV)

- Ultra-high vacuum (UHV) conditions → atomically clean surfaces

  the Flux, F, of molecules striking the surface of unit area at pressure P

  Z in (1.0.1)

- UHV ($<1.33 \times 10^{-7}$ Pa = 10^{-9} Torr) → to maintain a clean surface for ~ 1h
- Mean free path: distance that a particle travels on average between collisions → longer mean free path for electron in e^- spectroscopy

- UHV chamber & pumps

Light and electron sources

Electromagnetic radiation (light, photon)
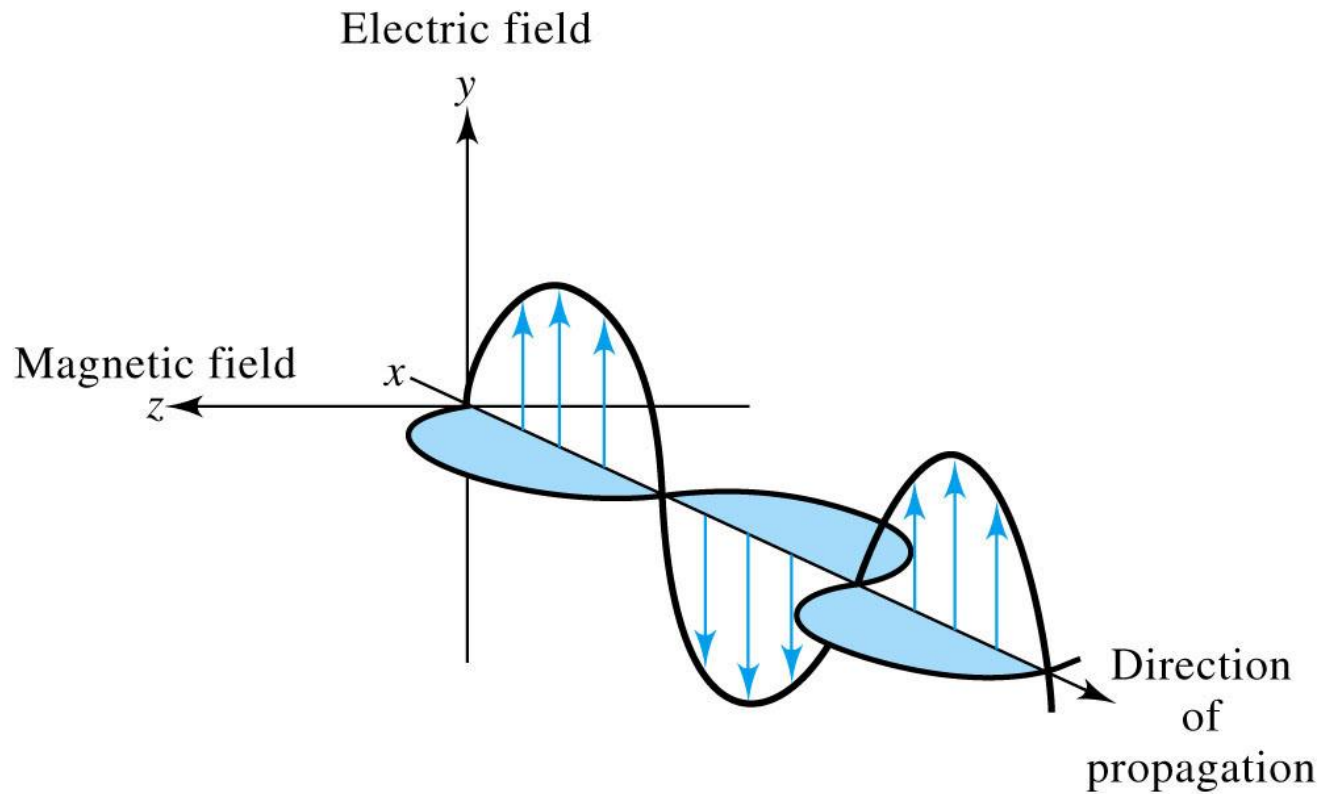
(a)

Electric component of electromagnetic wave
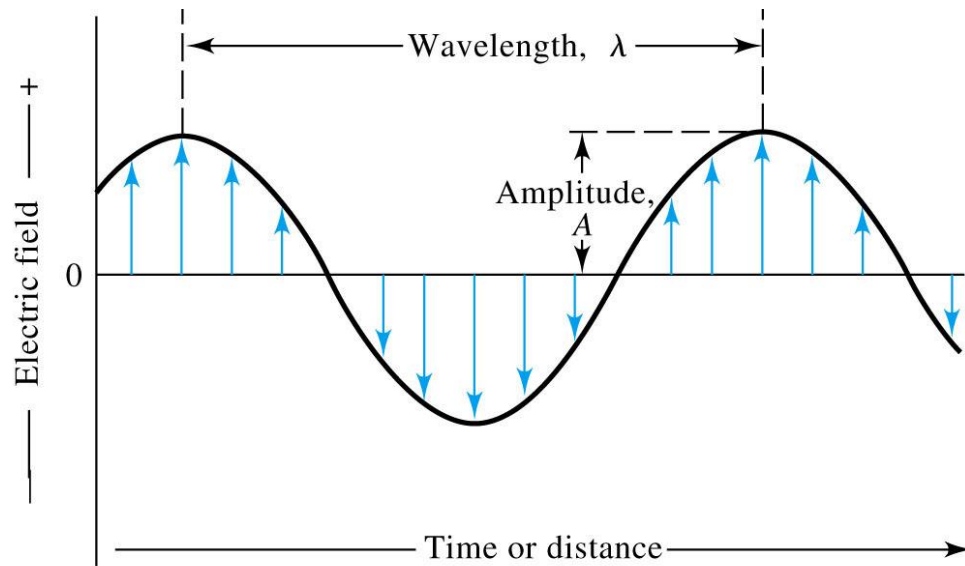
$$v_i = v\lambda_i \qquad (6\text{-}1)$$

velocity of propagation v_i
frequency v: number of
oscillations per second

In a vacuum, v_i is independent of wavelength and a maximum
$\rightarrow$ c = 2.99792 x 10^8 m/s

In a air, v_i differs only slightly from c (about 0.03% less): ~ c

$$c = v\lambda = 3.00 \times 10^8 \text{ m/s} = 3.00 \times 10^{10} \text{ cm/s} \qquad (6\text{-}2)$$

wavenumber $\bar{v}$: the reciprocal of wavelength in cm (cm^{-1})

The electromagnetic spectrum
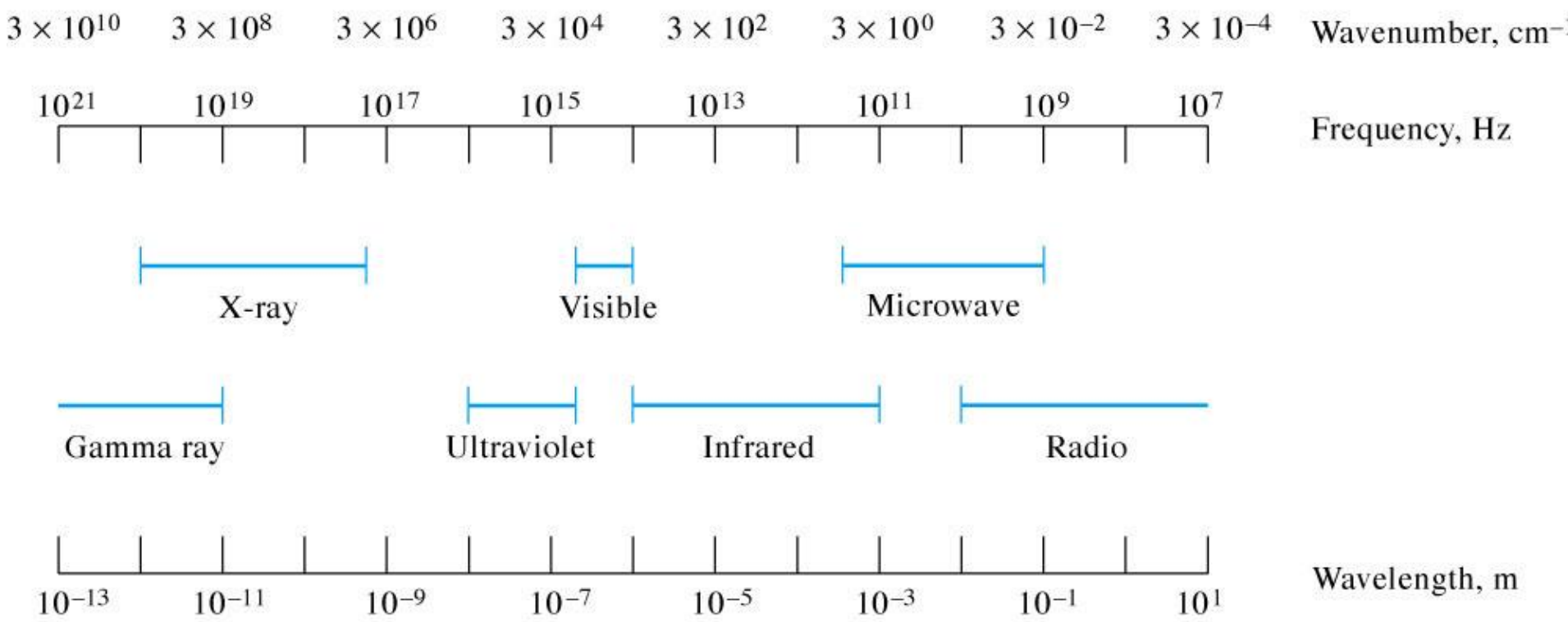
eV   nm   cm⁻¹   Hz

TABLE 6-1 Common Spectroscopic Methods Based on Electromagnetic Radiation

| Type of Spectroscopy	Usual Wavelength Range*	Usual Wavenumber Range, cm^{-1}	Type of Quantum Transition
Gamma-ray emission	0.005–1.4 Å	—	Nuclear
X-ray absorption, emission, fluorescence, and diffraction	0.1–100 Å	—	Inner electron
Vacuum ultraviolet absorption	10–180 nm	1×10^6 to 5×10^4	Bonding electrons
Ultraviolet-visible absorption, emission, and fluorescence	180–780 nm	5×10^4 to 1.3×10^4	Bonding electrons
Infrared absorption and Raman scattering	0.78–300 μm	1.3×10^4 to 3.3×10^1	Rotation/vibration of molecules
Microwave absorption	0.75–375 mm	13–0.03	Rotation of molecules
Electron spin resonance	3 cm	0.33	Spin of electrons in a magnetic field
Nuclear magnetic resonance	0.6–10 m	1.7×10^{-2} to 1×10^3	Spin of nuclei in a magnetic field

Types of lasers

Table 2.1 *Types of lasers and their characteristics including typical wavelengths, pulse durations, pulse energy or power, and repetition rates*

Laser material	λ/nm	$h\nu$/eV	Characteristics
Solid state			
Semiconductor laser diode	IR–visible $\sim$0.4–20 μm		Usually cw but can be pulsed, wavelength depends on material, GaN for short λ, AlGaAs 630–900 nm, InGaAsP 1000–2100 nm, used in telecommunications, optical discs
Nd^{3+}: YAG (1st harmonic)	1064	1.16	cw or pulsed, $\sim$10 ns pulses, most common, 150 ps versions (and shorter) available, 10–50 Hz rep rate, 1 J to many J pulse energies. Nd^{3+} can also be put in other crystalline media such as YLF(1047 and 1053 nm) or YVO_4 (1064 nm)
Nd^{3+}: YAG (2nd harmonic)	532	2.33	
Nd^{3+}: YAG (3rd harmonic)	355	3.49	
Nd^{3+}: YAG (4th harmonic)	266	4.66	
Nd^{3+}: glass	1062 or 1054	2.33	$\sim$10 ps, used to make terawatt systems for inertial confinement fusion studies
Ruby (Cr:Al_2O_3 in sapphire)	694	1.79	$\sim$10 ns
Ti:sapphire	700–1000	1.77–1.24	fs to cw; 1 Hz, kHz, 82 MHz
Alexandrite (Cr^{3+} doped $BeAl_2O_4$)	700–820	1.77–1.51	Tattoo removal
Liquid			
Dye laser	300–1000	4.13–1.24	Rep rate and pulse length depend on pump laser; fs, ps, ns up to cw
Gas			
CO_2	10 600 (10.6 μm)	0.12	Long (many μs), irregular pulses, cw or pulsed at high rep rates, line tuneable, few W to >1 kW
Kr ion	647	1.92	cw, line tuneable, 0.1–100 W
HeNe	632.8	1.96	cw, 0.5–35 W
	543.5	2.28	
Ar ion	514.5	2.41	cw, line tuneable, Ar and Kr ion laser (or versions with both present) are commonly used in the entertainment industry for light shows
	488	2.54	
HeCd	441.6, 325	2.81, 3.82	cw, 1–100 mW
ArF excimer	193	6.42	$\sim$20 ns, 1–>1000 Hz, several W to over 1 kW, 100 mJ to >1 J
KrF excimer	248	5.00	30–34 ns
XeCl excimer	308	4.02	22–29 ns
XeF excimer	351	3.53	12 ns
F_2	154	8.05	1–several kHz rep rate, 1–20 W, 10–50 mJ pulse energies, 10 ns
N_2	337	3.68	1–3.5 ns, 0.1–1+ mJ, 1–20 Hz rep rate

(continued overleaf)

X-ray

Electron

Characteristic X-rays

L-shell

K-shell

M-shell

Photo-electron
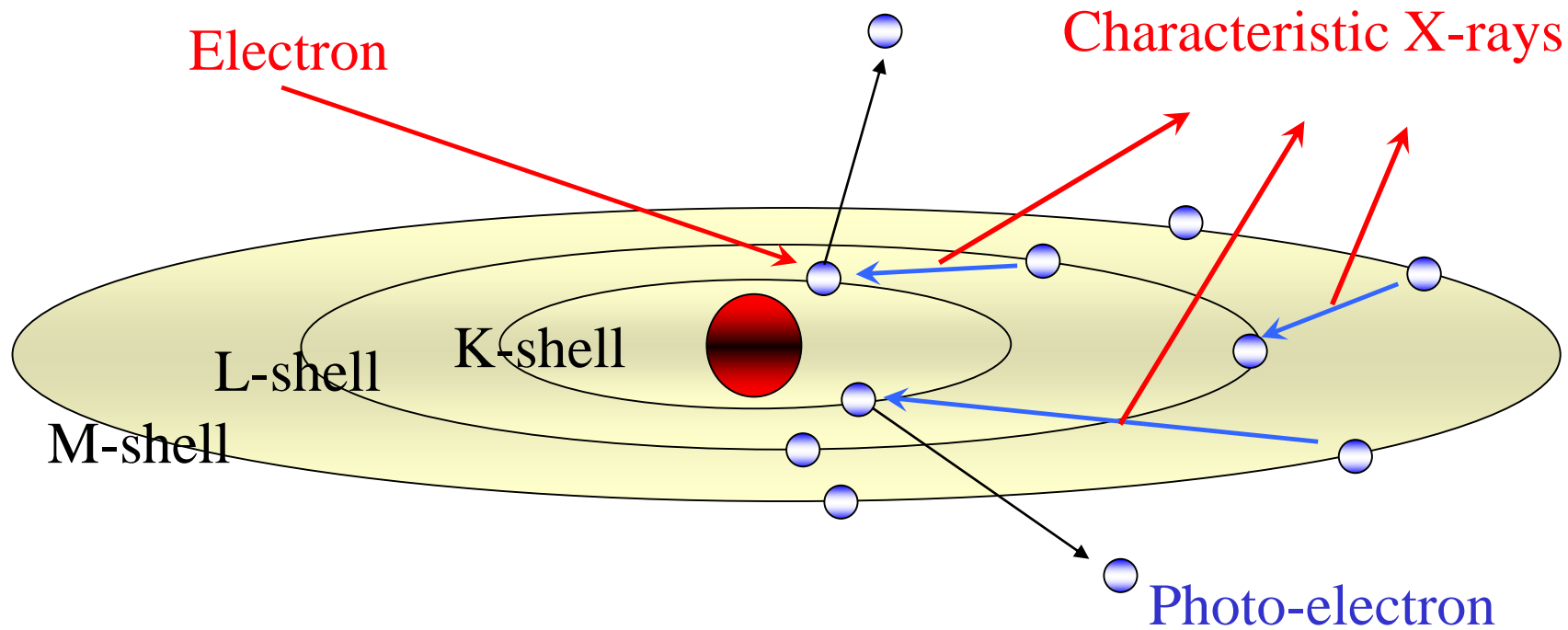
Synchrotron

X-ray absorption spectroscopy

Absorption edge (energy that is just need
to eject a particular core electron, e.g., 1s
(K edge), $2p_{3/2}$ e$^-$ (L$_3$ edge)

Fe & Fe oxides
K-edge: 7.112 keV

Within 10-40 eV: X-ray absorption
near-edge structure (**XANES**) (or near-ed
absorption fine structure (**NEXAFS**))
→ oxidation state & ligand environment

About 50 keV: extended X-ray absorption
Fine structure (**EXAFS**)
→ distance & arrangement of atoms
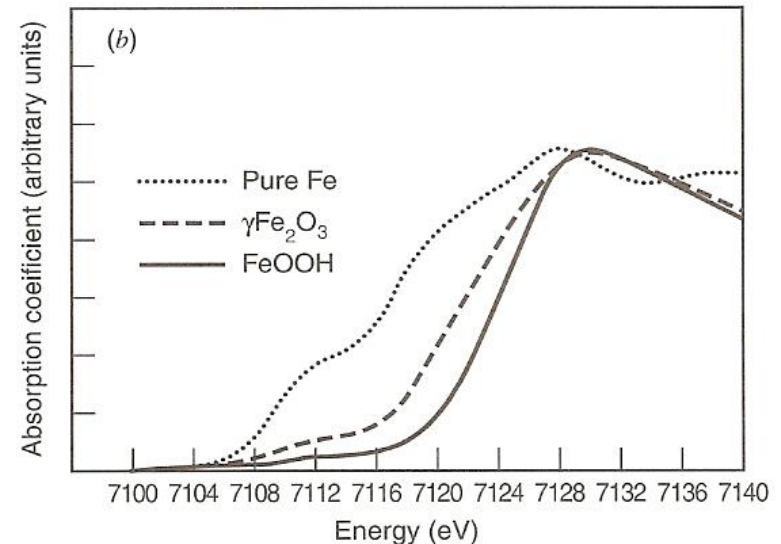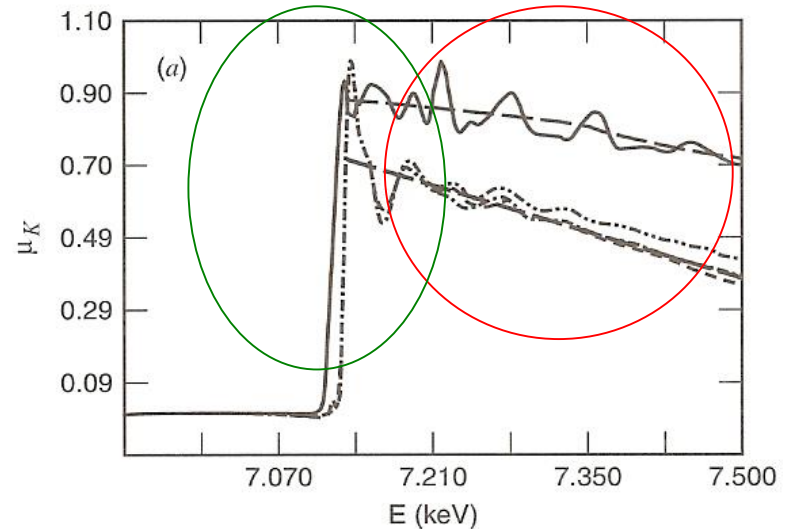
Spectroscopic surface methods

From source

To spectrometer

Photons, electrons, neutral molecules

Primary beam

Detected (secondary) beam

Photons, electrons, ions, molecules

Sample

© 2007 Thomson Higher Education
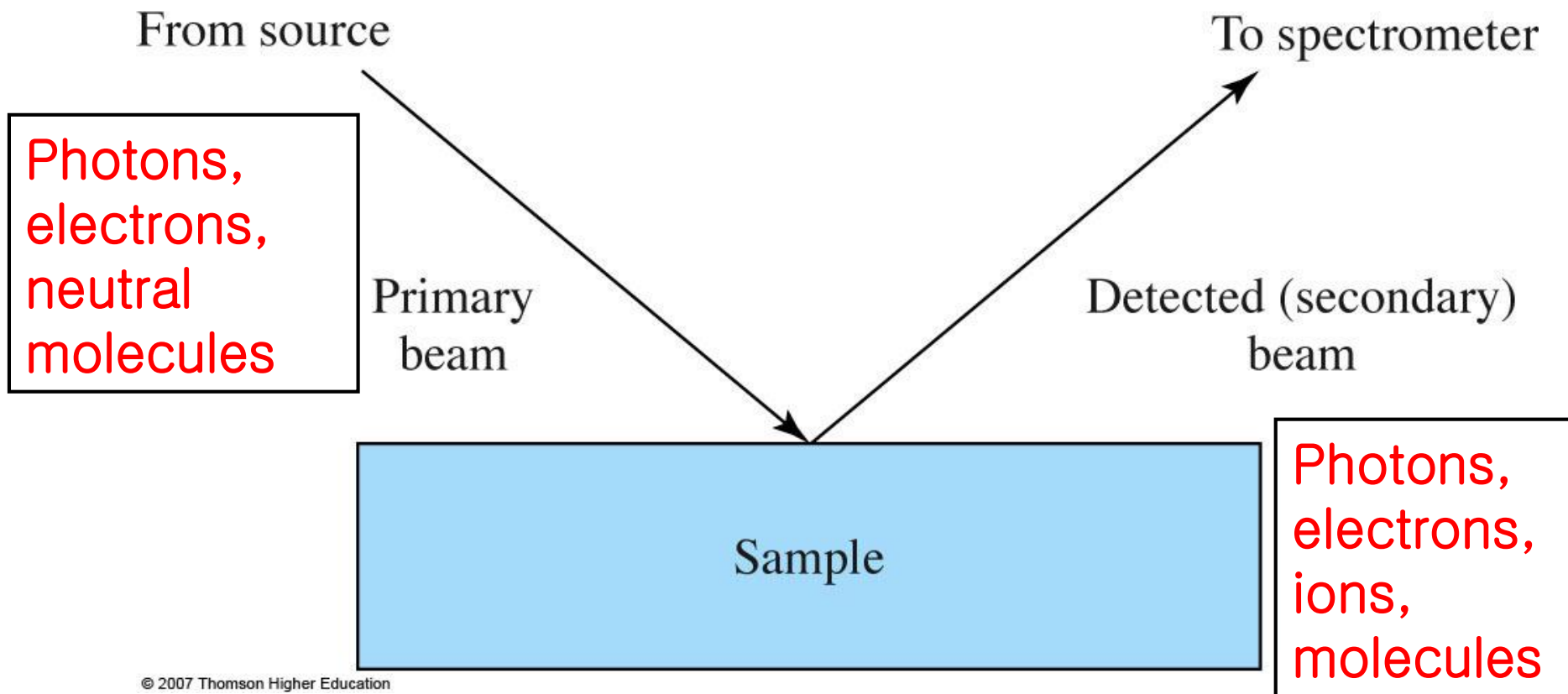
TABLE 21-1 Some Common Spectroscopic Techniques for Analysis of Surfaces

Method and Acronym	Primary Beam	Detected Beam	Information
X-ray photoelectron spectroscopy (XPS), or electron spectroscopy for chemical analysis (ESCA)	X-ray photons	Electrons	Chemical composition Chemical structure
Auger electron spectroscopy (AES)	Electrons or X-ray photons	Electrons	Chemical composition
Electron energy-loss spectroscopy (EELS)	Electrons	Electrons	Chemical structure Adsorbate binding
Electron microprobe (EM)	Electrons	X-ray photons	Chemical composition
Secondary-ion mass spectrometry (SIMS)	Ions	Ions	Chemical composition Chemical structure
Ion-scattering spectroscopy (ISS) and Rutherford backscattering	Ions	Ions	Chemical composition Atomic structure
Laser-microprobe mass spectrometry (LMMS)	Photons	Ions	Chemical composition Chemical structure
Surface plasmon resonance (SPR)	Photons	Photons	Composition and concentration of thin films
Sum frequency generation (SFG)	Photons	Photons	Interface structure, adsorbate binding
Ellipsometry	Photons	Photons	Thin-film thickness

Electron and ion
Ultra high vacuum (UHV)
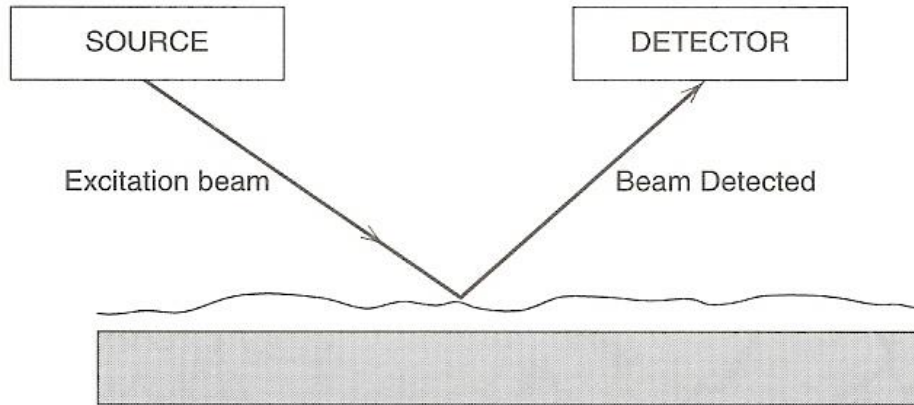
	Excitation	Detection
X-ray photoelectron spectroscopy (XPS)	Photons(X-ray)	Electrons
UV photoelectron spectroscopy (UPS)	Photons (UV)	Electrons
Auger electron spectroscopy (AES)	Electrons	Electrons
Low-energy electron diffraction (LEED)	Electrons	Electrons
High resolution e⁻ E loss spec. (HREELS)	Electrons	Electrons
Rutherford backscattering (RBS)	H+ or He+	H+ or He+
Secondary ion mass spec. (SIMS)	Ions	Ions
Laser desorption mass spec. (LDMS)	Photons	Ions

Scanning probe techniques

Microscopy: a sharp tip close to the surface → scanning electron or force and so on → STM, AFM and so on

Similar idea: NSOM (Near field scanning optical microscopy) → a small-diameter optical fiber close to the surface (diameter/distance < wavelength of the light) → image resolution far below light wavelength

SP techniques: current, van der Waals force, chemical force, magnetic force, capacitance, phonon, photon

UHV or at atmosphere or in solution, *in situ vs. ex situ* techniques

Scanning tunneling microscopy (STM)
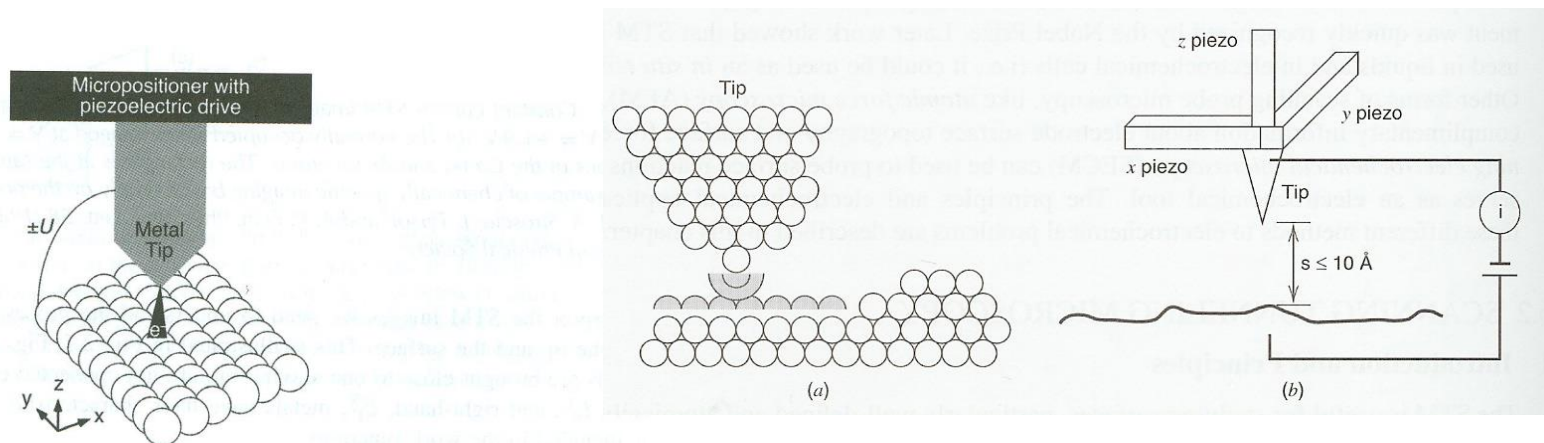
Figure 2.3 *Schematic drawing of a scanning tunnelling microscope tip interacting with a surface.*

Tunnelling

- if the potential energy of a particle does not rise to infinite in the wall &
    $E < V \rightarrow \Psi$ does not decay abruptly to zero
- if the walls are thin $\rightarrow \Psi$ oscillate inside the box & on the other side of
    the wall outside the box $\rightarrow$ particle is found on the outside of a
    container: leakage by penetration through classically forbidden
    zones "tunnelling"
cf) C.M.: insufficient energy to escape
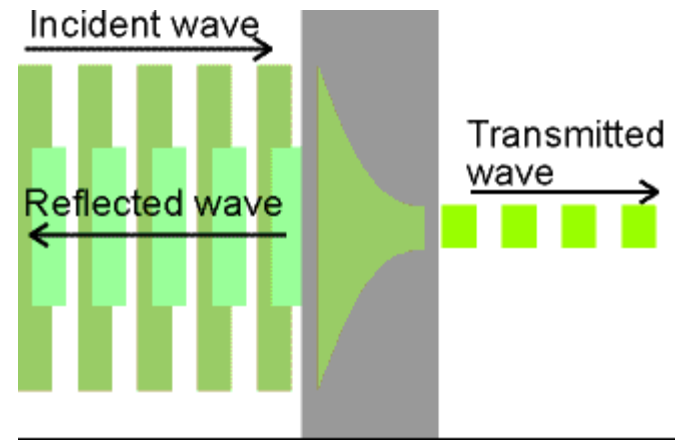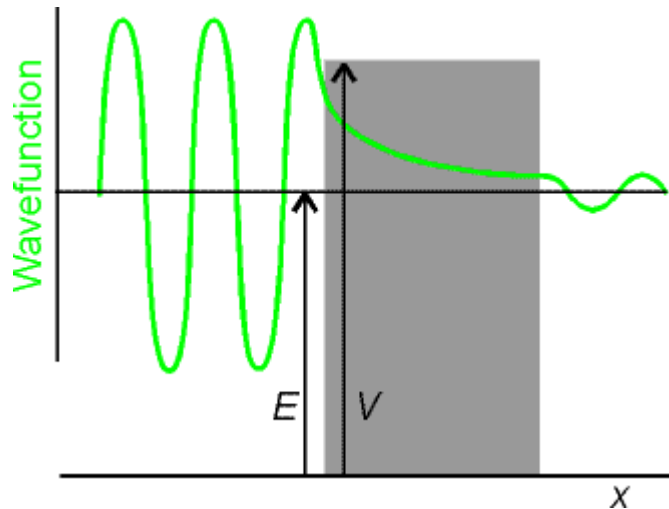
$\Rightarrow$ T decrease exponentially with thickness of the barrier, with m$^{1/2}$

$\Rightarrow$ low mass particle $\rightarrow$ high tunnelling *tunnelling is important for electron
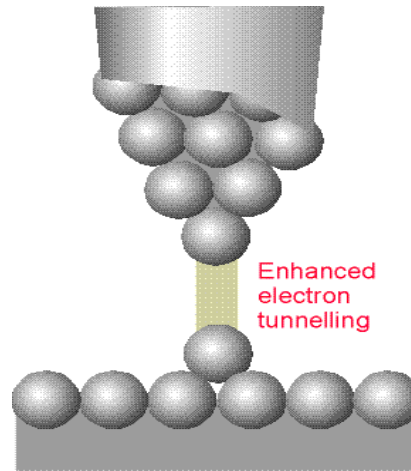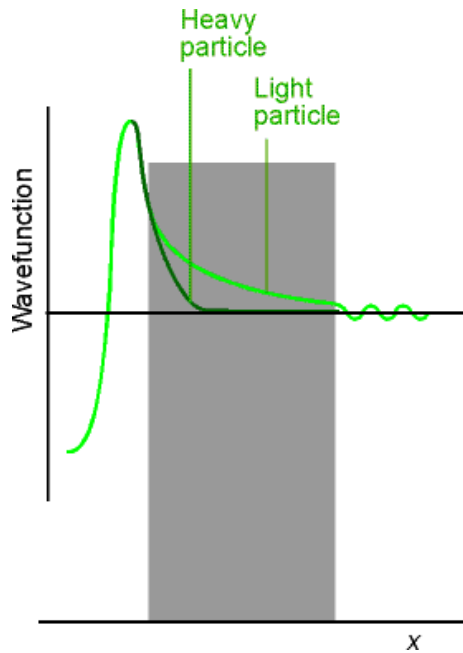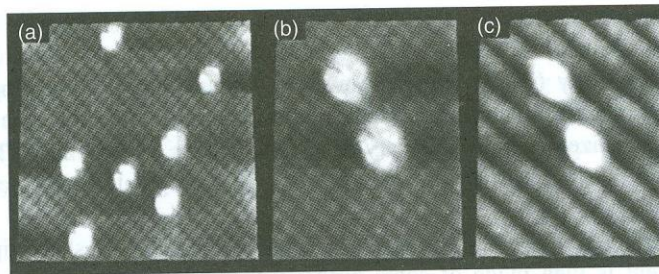
Figure 2.4 An STM image of occupied states on a Si(100)–(2 × 1) surface nearly completely covered with adsorbed H atoms. The uncapped Si dangling bonds (sites where H is not adsorbed) appear as lobes above the plane of the H-terminated sites. The rows of the (2 × 1) reconstruction are clearly visible in the H-terminated regions. Reproduced from J. J. Boland, Phys. Rev. Lett. *65* (1990) 3325. © 1990, with permission from the American Physical Society.
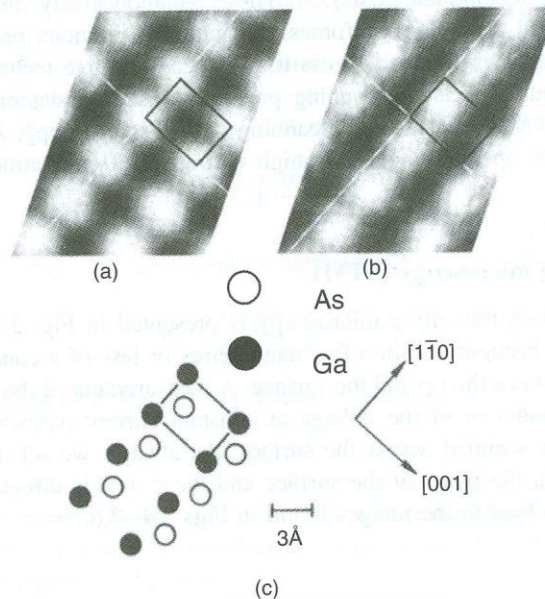
Figure 2.5 Constant current STM images of the clean GaAs(110) surface. (a) The normally unoccupied states imaged at $V = +1.9\,V$. (b) The normally occupied states imaged at $V = -1.9\,V$. (c) Schematic representation of the positions of the Ga (●) and As (o) atoms. The rectangle is at the same position in (a), (b) and (c). This is an unusual example of chemically specific imaging based simply on the polarity of the tip. Reproduced from R. M. Feenstra, J. A. Stroscio, J. Tersoff and A. P. Fein, Phys. Rev. Lett. *58* (1987) 1192. ©1987, with permission from the American Physical Society.
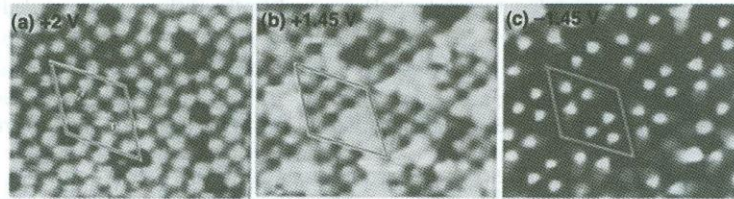
Figure 2.6 *Constant current STM images of the Si(111)–(7 × 7) surface. Notice how the apparent surface structure changes with voltage even though the surface atom positions do not change. This illustrates that STM images electronic states (chosen by the voltage) and not atoms directly. Reproduced from R. J. Hamers, R. M. Tromp and J. E. Demuth, Phys. Rev. Lett. 56 (1986) 1972. © 1986, with permission from the American Physical Society.*
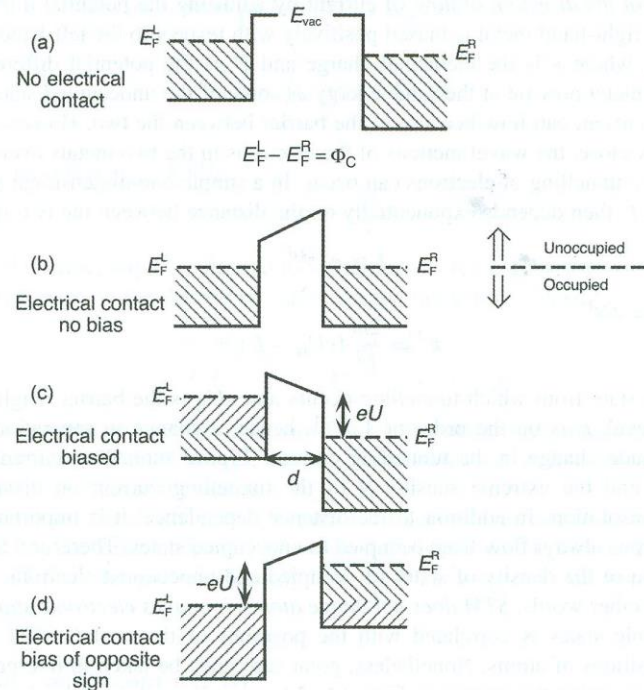

Figure 2.7 *Illustrations of the Fermi and vacuum level positions for two metals separated by distance d. (a) Isolated metals. (b) After electrical contact, in the absence of an applied bias. (c) Biasing shifts the relative positions of the Fermi levels and makes available unoccupied states in an energy window eU into which electrons can tunnel. (d) The direction of tunnelling is switched compared to the previous case simply by changing the sign of the applied bias. Adapted from J. Tersoff, N. D. Lang, Theory of scanning tunneling microscopy, in Scanning Tunneling Microscopy (Eds J. A. Stroscio, W. J. Kaiser), Academic Press, Boston, 1993, p. 1. © 1993, with permission from Academic Press.*

Electrochemical STM
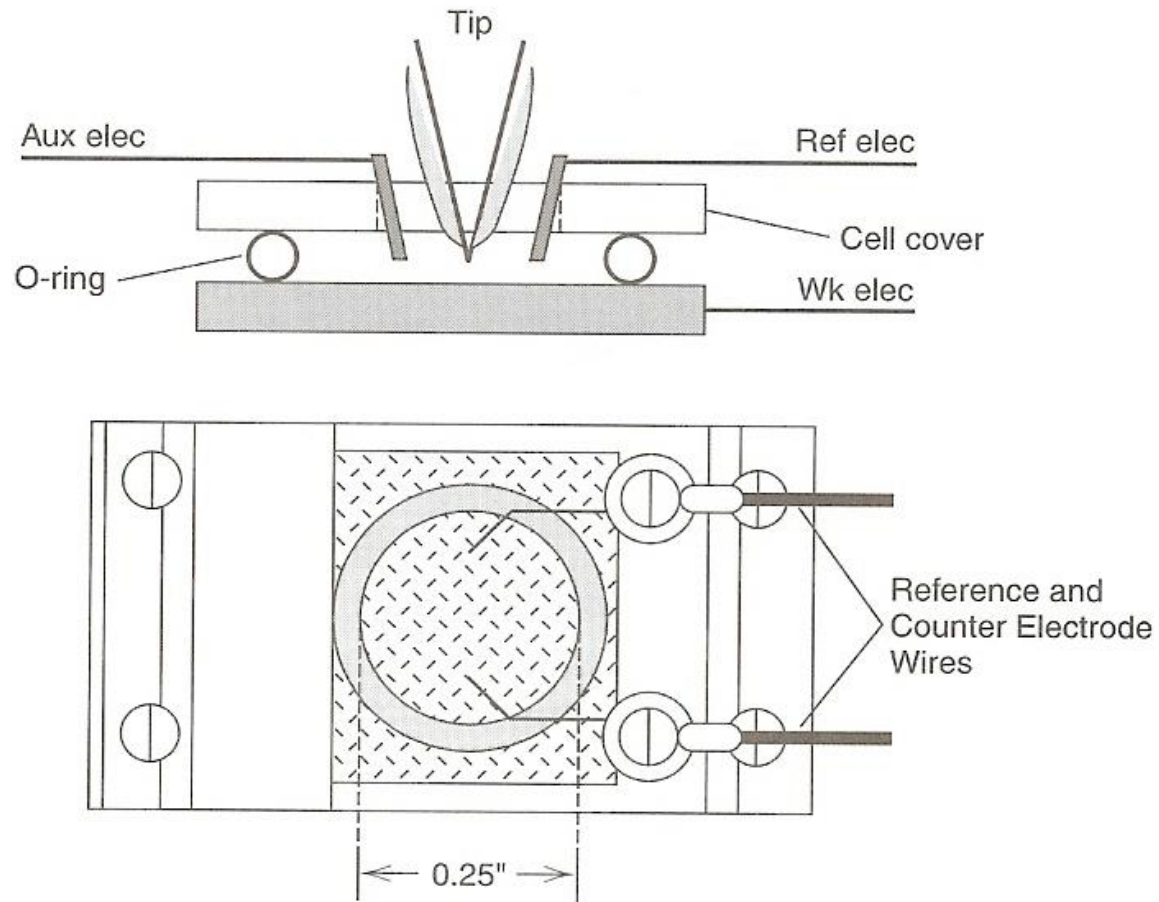
Scanning tunneling spectroscopy (STS)

STM image depends on the voltage
on the tip → control of the voltage
→ to determine the electronic states
with atomic resolution (STS)
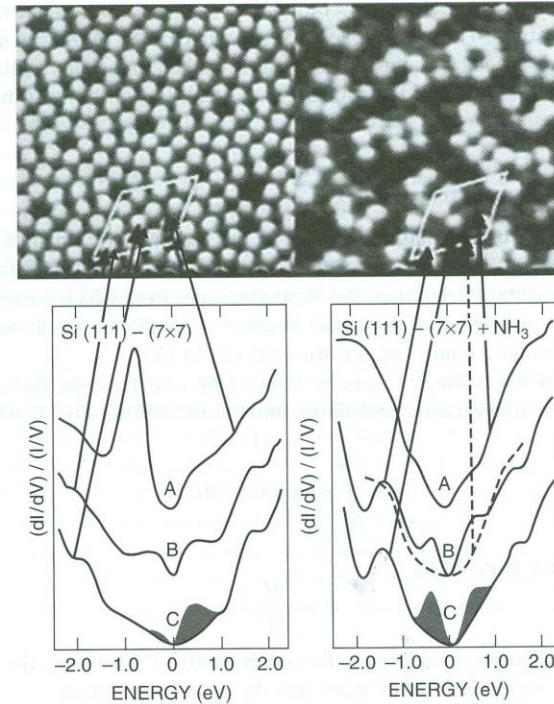
Figure 2.8 *Left-hand side: Topography of the unoccupied states of the clean (7 × 7) surface (top panels) and atom resolved tunnelling spectra (bottom panels). The curves represent spectra acquired over different sites in the reconstructed surface (Curve A: restatom, Curve B: corner adatom, Curve C: middle adatom). Negative energies correspond to occupied states, positive to empty states. Right-hand side: Same types of images and spectra obtained after exposure of a Si(111)–(7 × 7) surface to NH₃. The different sites exhibit different reactivities with respect to NH₃ adsorption with the restatoms being the most reactive and the middle adatoms being the least reactive. Reproduced from R. Becker and R. Wolkow, Semiconductor surfaces: Silicon, in Scanning Tunnelling Microscopy (Eds J. A. Stroscio, W. J. Kaiser), Academic Press, Boston, 1993, p. 193. © 1993, with permission from Academic Press.*

Table 2.2 *Interaction forces appropriate to scanning force microscopy and their ranges. Values taken from Takano et al. [32]*

| Force	Range (nm)
Electrostatic	100
Double layer in electrolyte	100
van der Waals	10
Surface-induced solvent ordering	5
Hydrogen bonding	0.2
Contact	0.1

AFM

Atomic force microscopy (AFM)
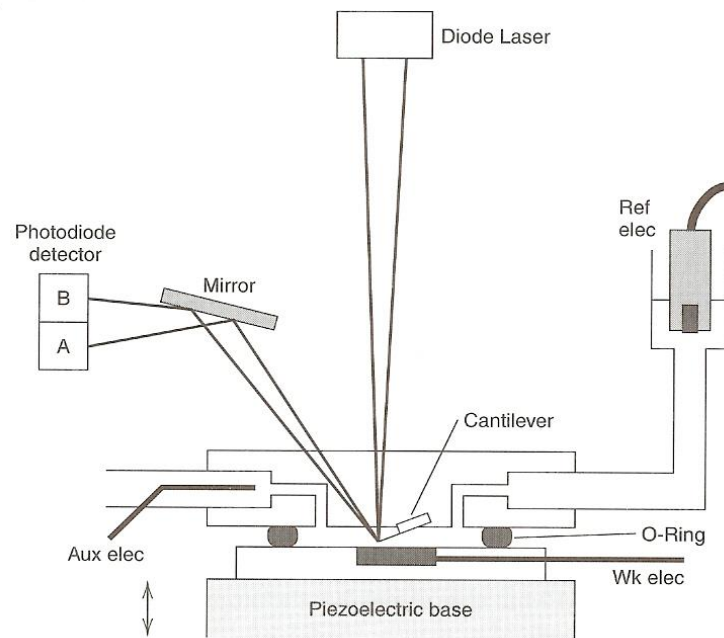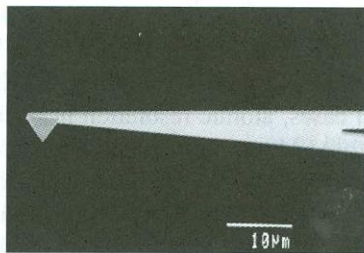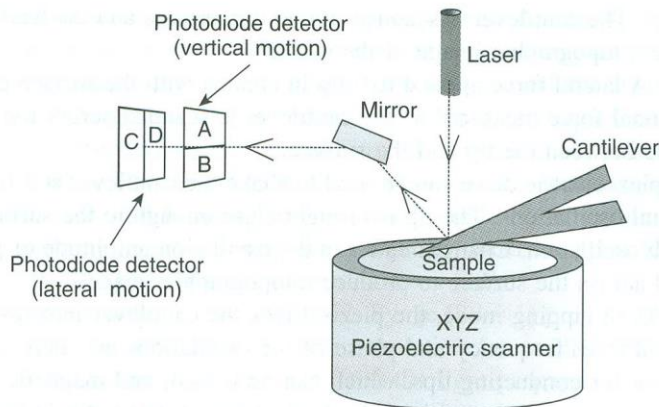
Figure 2.9 *Principal components for an optical lever type AFM. Detection of the reflected laser beam with a quadrant, position sensitive photodiode facilitates the simultaneous detection of bending and torsion of the cantilever. A scanning electron micrograph of a typical AFM cantilever and tip is shown in the lower panel. Reproduced from H. Takano, J. R. Kenseth, S.-S. Wong, J. C. O'Brien, M. D. Porter, Chem. Rev. 99 (1999) 2845. © 1999, with permission from the American Chemical Society.*

Scanning electrochemical microscopy (SECM)
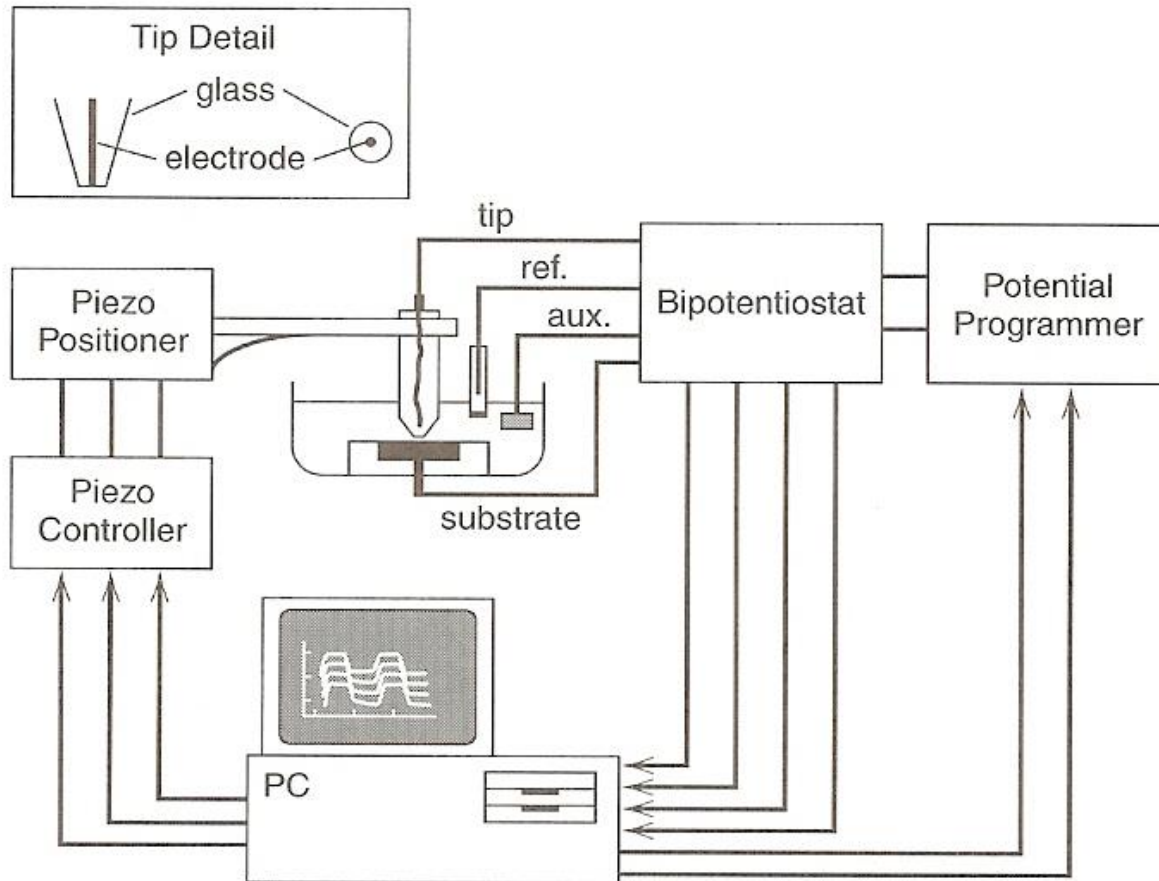
Optical and electron microscopy

Optical microscopy

• Limit of resolution(δ): mainly by the wavelength λ of the light

$$\delta = \lambda / 2n \sin \alpha$$

α: the angular aperture (half the angle subtended at the object by the objective lens),
n: the refractive index of the medium between the object and the objective lens,
n sin α: the numerical aperture of the objective lens for a given immersion medium

Numerical aperture: generally less than unity
　　　　　　　　　up to 1.5 with oil-immersion objectives → 600 nm light: 200 nm
　　　　　　　　　　　　　　　　　　　　　　　　　(0.2 μm) resolution limit
Serious error in particle size less than 2 μm (Table 3.1)

Table 3.1 Determination of the diameters of spherical particles by optical micro-scopy[29]

True diameter/μm	Visual estimate/μm
1.0	1.13
0.5	0.68
≤ 0.2	0.5

• Limitation: resolution power & contrast

Transmission electron microscopy(TEM)

- e-beam: wavelength $\lambda \sim 0.01$ nm
- resolution: 0.2 nm
- limitation: high vacuum system

Scanning electron microscopy(SEM)

- resolution: ~ 5 nm

SEM
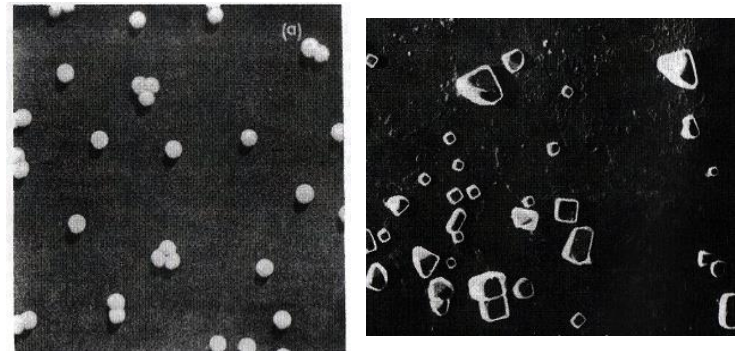
Figure 3.2 Electron micrographs. (a) Shadowed polystyrene latex particles (×50 000). (b) Shadowed silver chloride particles (× 15 000)

Near-field scanning optical microscopy (NSOM or SNOM)

a small-diameter optical fiber close to the surface (diameter/distance
< wavelength of the light) → image resolution far below light wavelength

Optical fiber + laser + AFM techniques
Resolution ~ 50 nm, ultimate resolution ~ 12 nm
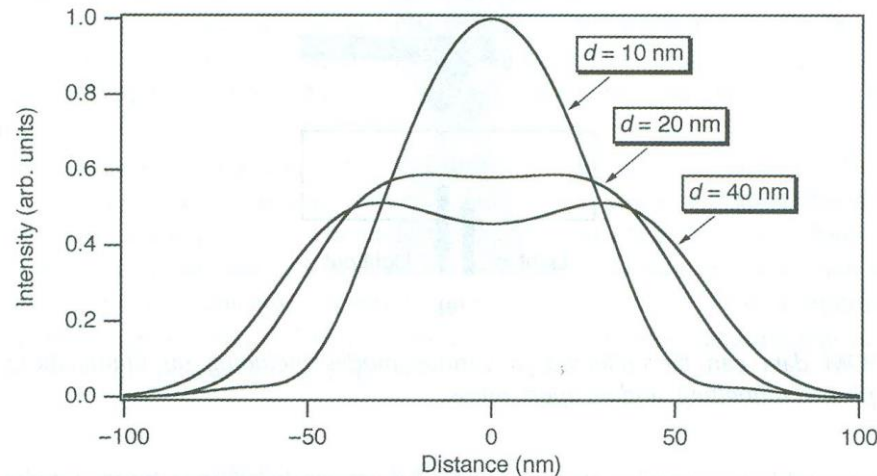
Figure 2.10 *Near-field intensity distributions are shown for 532 nm light that has passed through an aperture with a diameter of 100 nm at distances d from the aperture of 10, 20 and 40 nm. The distributions are normalized such that they all have the same integrated intensity.*
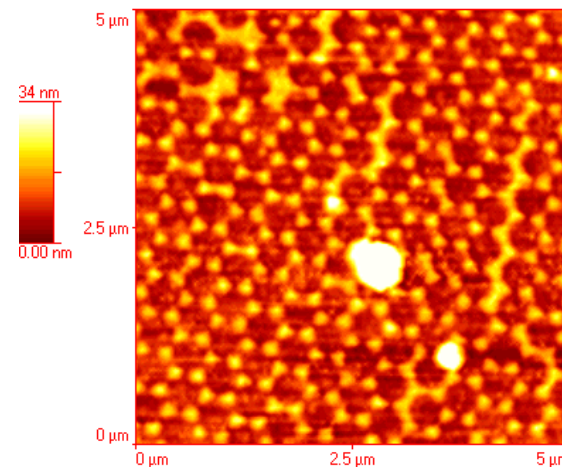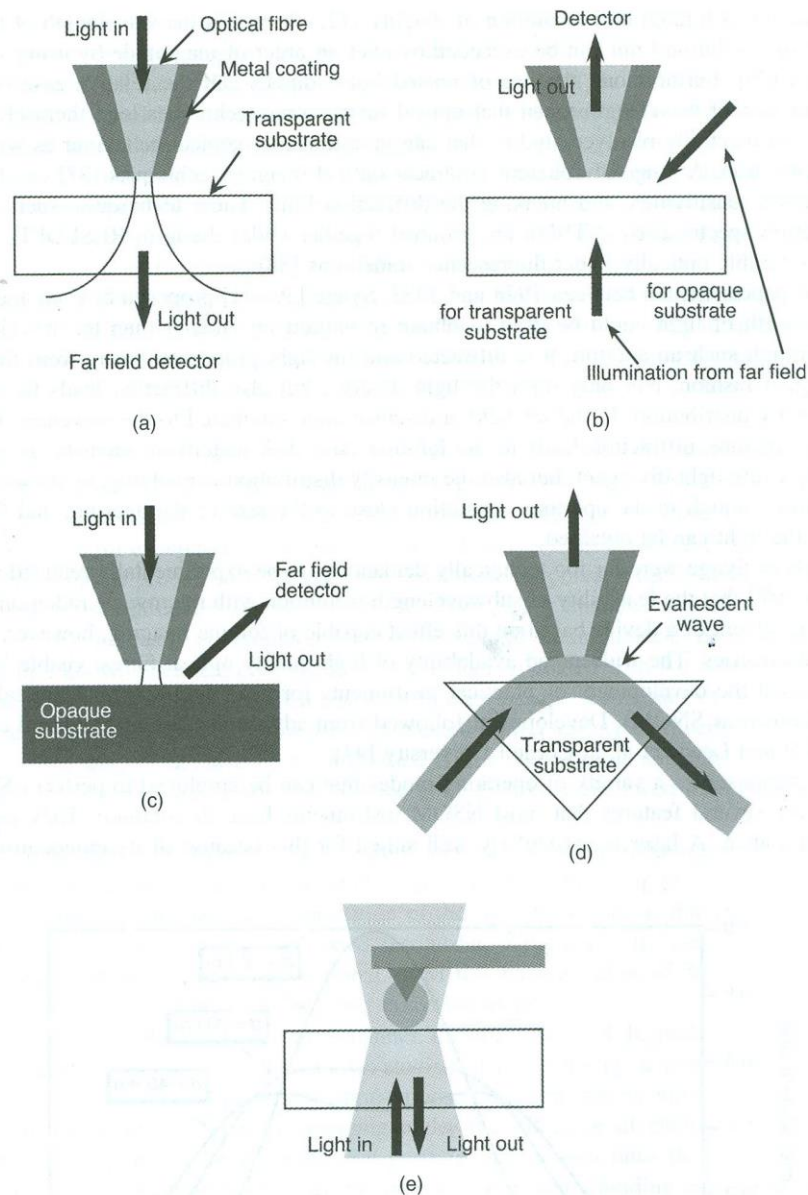
Figure 2.11 *NSOM data can be collected in various modes including (a) illumination; (b) collection; (c) reflection; (d) photon tunnelling; and (e) apertureless.*

elchem.kaist.ac.kr

Low energy electron diffraction (LEED)
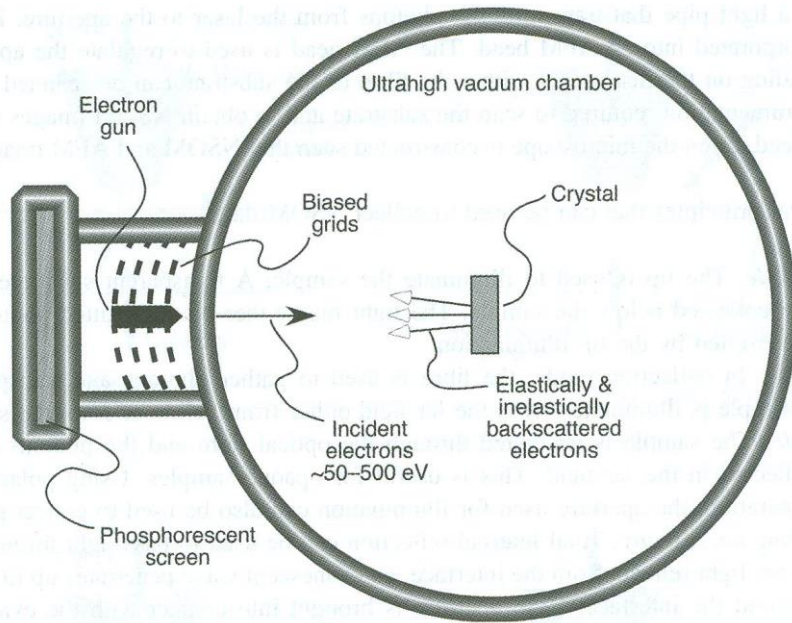
Figure 2.12 *Schematic drawing of a LEED chamber.*

Ultrahigh vacuum chamber

Electron gun

Biased grids

Crystal

Incident electrons ~50–500 eV

Elastically & inelastically backscattered electrons

Phosphorescent screen
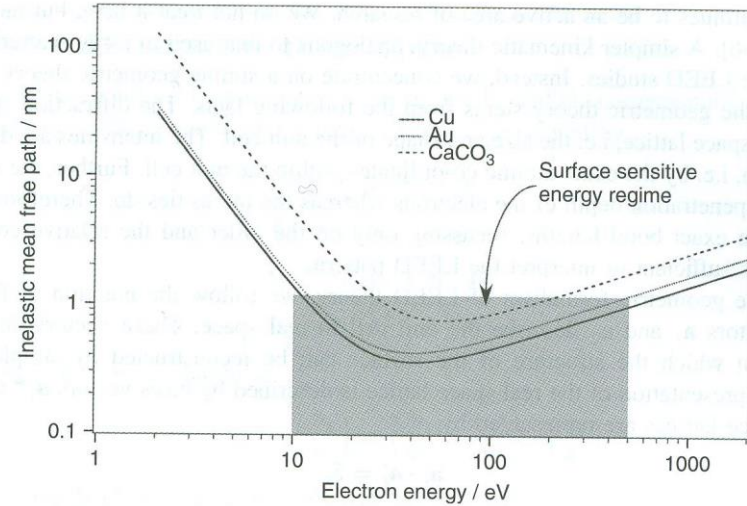
universal curve of electron mean free path λ in solid matter. Calculated from the data of Seah

Inelastic mean free path / nm

Electron energy / eV

— Cu
---- Au
···· CaCO₃

Surface sensitive energy regime

Surface diffraction

- Low energy electron diffraction (LEED), X-ray diffraction, atomic diffraction

de Broglie wavelength, λ, of a particle $\lambda = h/p$

$$\lambda = \frac{h}{\sqrt{2mE}} \tag{2.1}$$

where h is Planck's constant, m is the mass of the particle, and E is the kinetic energy of the particle. For electrons and He atoms, Eq. 2.1 is more conveniently expressed as:

$$\lambda_{e^-}(\text{Å}) = \sqrt{\frac{150}{E\,(\text{eV})}} \quad \text{and} \quad \lambda_{\text{He}}(\text{Å}) = \sqrt{\frac{0.02}{E\,(\text{eV})}} \tag{2.2}$$

For X-rays, the wavelength of a photon is given by

$$\lambda_{\text{photon}}(\text{Å}) \approx \frac{1.24 \times 10^4}{E\,(\text{eV})} \tag{2.3}$$

Electrons with 10~200 eV energies and He atoms with thermal energies (~0.026 eV at 300K) → atomic diffraction condition (λ < interatomic distance, ~1 Å)

X-rays at the high intensities available at a synchrotron radiation suitable for surface and interface structure studies (grazing angle X-ray diffraction). X-ray bombardment-induced emission of electrons also shows diffraction (photoelectron diffraction)

LEED: electron beam of 10~200 eV is back-scattered → atomic structure of surface
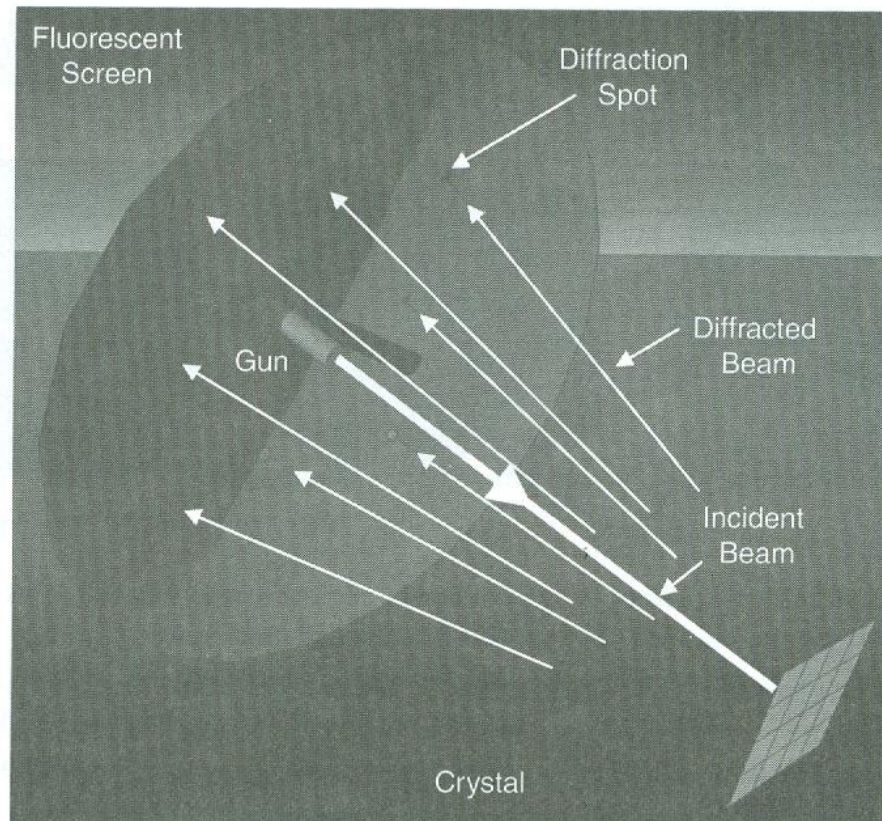
Figure 2.7. A scheme illustration of LEED surface crystallography.

Low energy electron diffraction (LEED):

Why low energy electron used?

- The penetration depth of x-ray is ~ 1µm. So x-ray diffraction give structural information of a bulk solid (3D). It does not have any surface sensitivity
- The penetration depth of low energy electron is ≤ 20 Å; a rather good surface sensitivity
- In any diffraction the employed wavelength λ should ~ d

- De Broglie wavelength of **e⁻** is
$$\lambda = h/p = h/mv = h/(2mE_k)^{1/2}$$

If $E_k = 150$ eV, $\lambda =\sim 1$ Å

- Since diffraction can be observed in elastic scattering, the inelastically scattered electrons have to be removed by setting up an potential barrier (grid assembly).
- The LEED pattern is usually recorded by taking a picture.
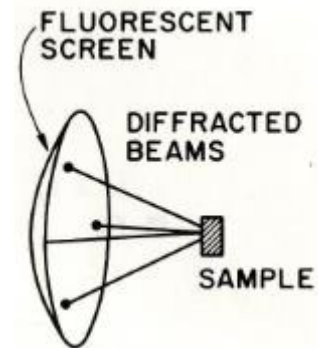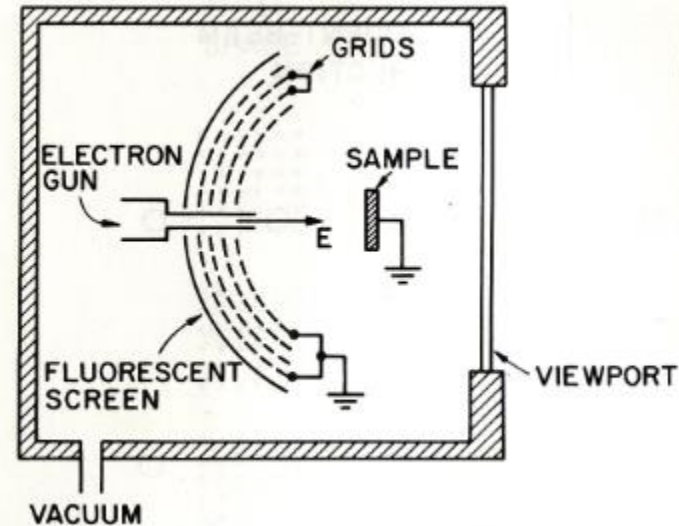
Instrument

Reciprocal lattice

The inverse relationship between real and reciprocal space means that a long vector in real space corresponds to a short vector in reciprocal space

$$b_1 = m_{11} a_1 + m_{12} a_2$$

in matrix notation,

$$b = \mathfrak{M} \cdot a \qquad \mathfrak{M} = \begin{pmatrix} m_{11} & m_{12} \\ m_{21} & m_{22} \end{pmatrix}$$

$$b_2 = m_{21} a_1 + m_{22} a_1$$
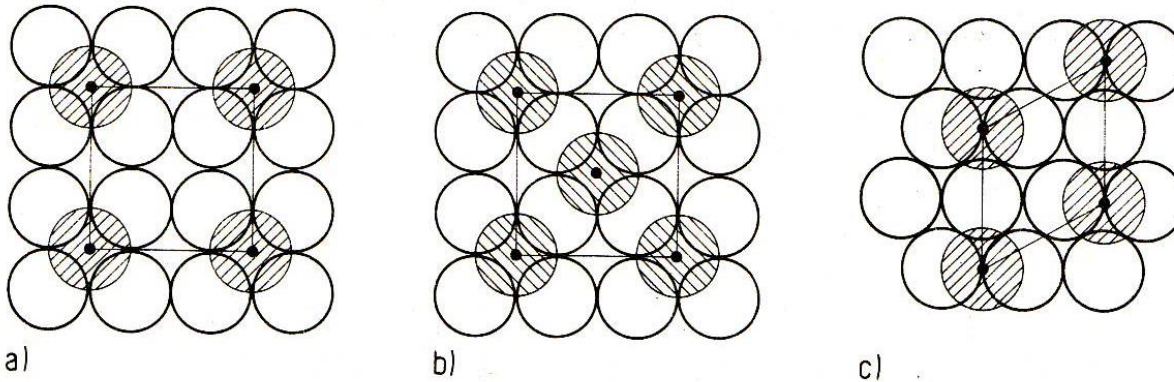
Fig. 9.2. Examples for overlayer structures. a) 2×2, b) $c(2 \times 2)$, c) $\sqrt{3} \times \sqrt{3}/R\,30°$.

$$\mathfrak{M} = \begin{pmatrix} 2 & 0 \\ 0 & 2 \end{pmatrix}, \begin{pmatrix} 1 & 1 \\ -1 & 1 \end{pmatrix} \text{ and } \begin{pmatrix} 1 & 1 \\ -1 & 2 \end{pmatrix}$$

2D real vs. reprociprocal lattices

$$b_1 = m_{11}a_1 + m_{12}a_2 \qquad b_1^* = m_{11}^* a_1^* + m_{12}^* a_2^*$$
$$b_2 = m_{21}a_1 + m_{22}a_2 \ . \qquad b_2^* = m_{21}^* a_1^* + m_{22}^* a_2^* \ .$$

m_{ij}^* can be measured directly from LEED pattern

$\mathfrak{M}* = \widetilde{\mathfrak{M}}^{-1}$, and so $\mathfrak{M} = \widetilde{\mathfrak{M}}*^{-1}$

m*: inverse transposed matrix of m
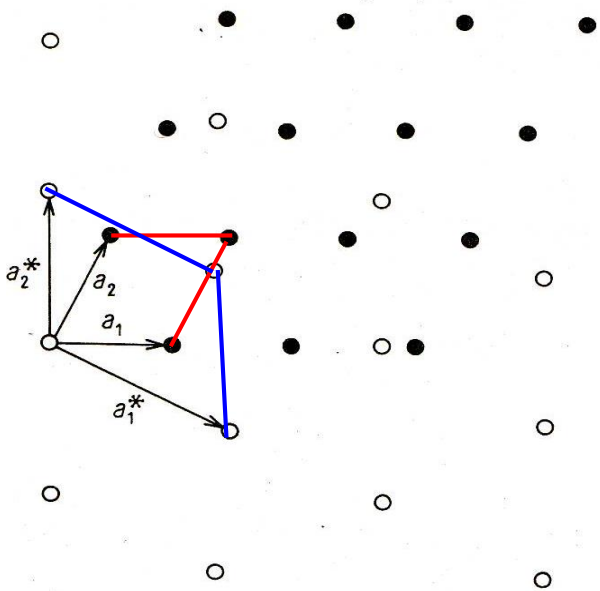
$$m_{11} = \frac{1}{\det \mathfrak{M}*} \cdot m_{22}^*$$

$$m_{12} = -\frac{1}{\det \mathfrak{M}*} \cdot m_{21}^*$$

$$m_{21} = -\frac{1}{\det \mathfrak{M}*} \cdot m_{12}^*$$

$$m_{22} = \frac{1}{\det \mathfrak{M}*} \cdot m_{11}^*$$

where det $\mathbf{m}^* = m_{11}^* \cdot m_{22}^* - m_{21}^* \cdot m_{12}^*$

Fig. 9.11. A two-dimensional real lattice, described by a_1, a_2 (dark circles), and its reciprocal lattice a_1^*, a_2^* (open circles).

$\mathfrak{M}* = \widetilde{\mathfrak{M}}^{-1}$, and so $\mathfrak{M} = \widetilde{\mathfrak{M}}*^{-1}$

Bragg reflection
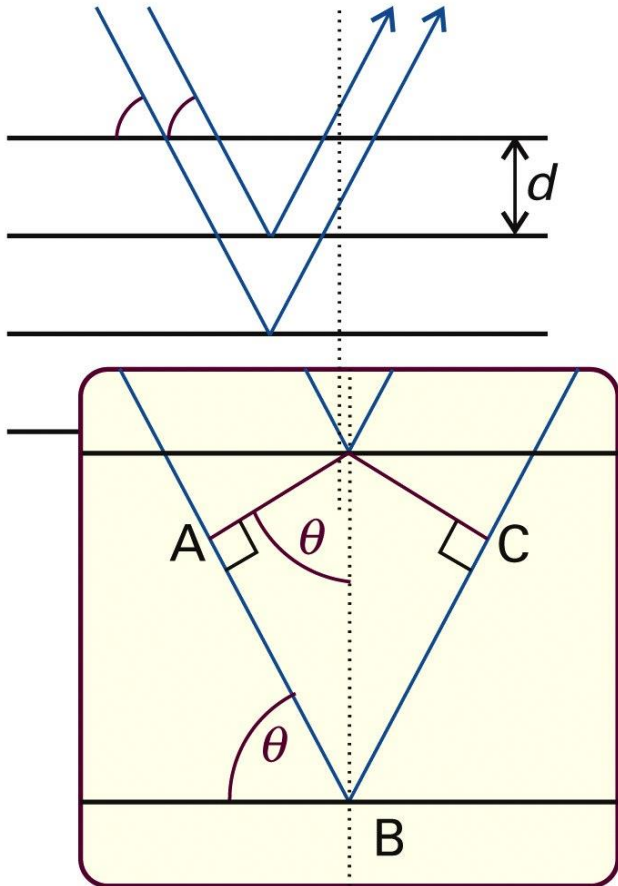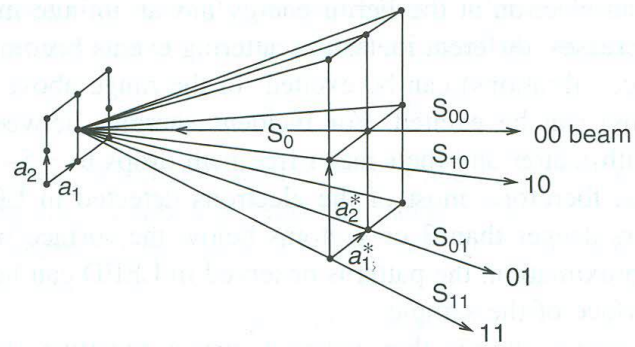
Figure 2.14 *The principle of diffraction pattern formation in a LEED experiment. The incident electron beam approaches along s_0. The specular beam exits along s_{00}. Reproduced from G. Ertl, J. Küppers,* Low Energy Electrons and Surface Chemistry, *2nd ed., VCH, Weinheim. © 1985, with permission from John Wiley & Sons, Ltd.*

01 a_2^* 11
b_2^*
00 10
b_1^* a_1^*

b_2

b_1

a_2 γ
a_1

(a) Reciprocal space

● Overlayer
○ Substrate

(b) Real space $c(4 \times 2)$

◉ Overlayer
○ Substrate
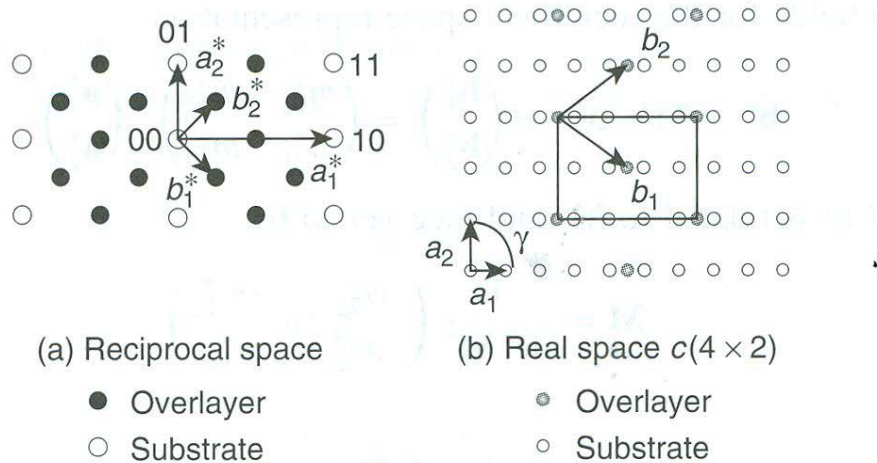
Figure 2.15 *Real space and reciprocal space patterns. (a) Reciprocal lattice (LEED pattern) composed o substrate (normal) spots ○ and overlayer (extra) spots ●. (b) Real lattice of the substrate (○) and overlayer (◉) The solid line delineates the $c(4 \times 2)$ cell and the arrows depict the unit vectors.*

LEED image

Bisulfate/Pt(111)
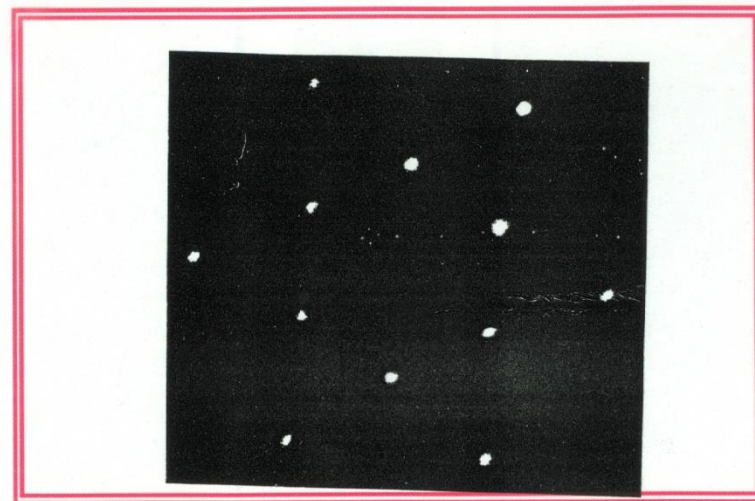
E = 0.34 V in 50 mM sulfuric acid   49.4 eV
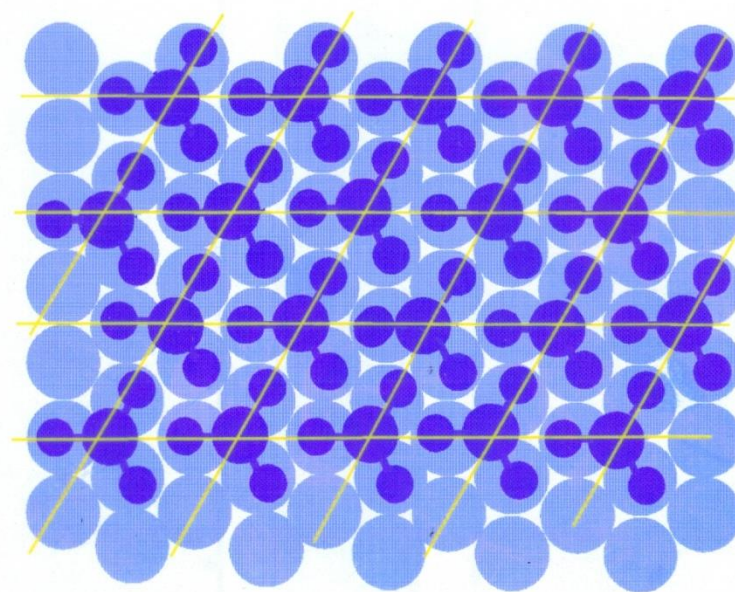
$(\sqrt{3} \times \sqrt{3})R30°$

Electron spectroscopy

XPS, UPS, AES
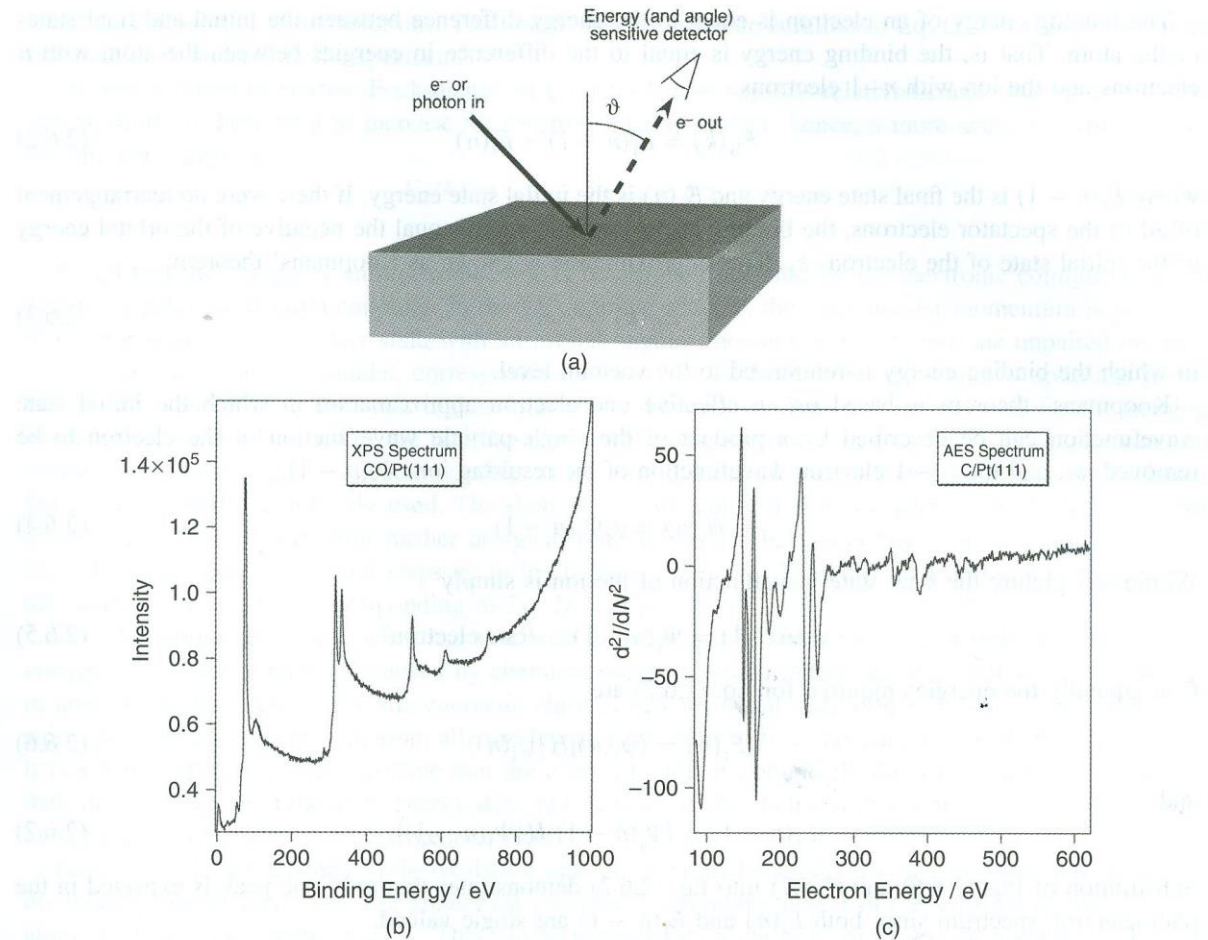
Figure 2.17 (a) Schematic representation of electron spectroscopy. (b) A sample XPS spectrum of CO/Pt(111). (c) A sample AES spectrum of CO/Pt(111).

X-ray photoelectron spectroscopy (XPS)
or electron spectroscopy for chemical analysis (ESCA)

$$E_b = hv - E_k - w \qquad (21\text{-}2)$$

$$E_k \approx h \qquad E_b$$

Photoelectrons

E'' ──────────

E' ──────────

E ──────────

Decreasing binding energy →

X-ray h

e

E_b'' ──────────

E_b' ──────────

E_b ──────────

© 2007 Thomson Higher Education

(a)

X-ray source

$h\nu$

E_k

Detection

Sample

$n = 3, 2, 1$

(b)

Number of counts

2s

2p

3s

3p

3d

0

$\longleftarrow$ E Binding energy/Kinetic energy $\longrightarrow$

$(C_3H_7)_4N^+S_2PF_2^-$

Counting rate

Binding energy

F_{1s}

Fluorine
Auger

O_{1s}

N_{1s}

C_{1s}

S_{2s}

P_{2s}

S_{2p}

P_{2p}

Survey scan

800   700   600   500   400   300   200   100   eV
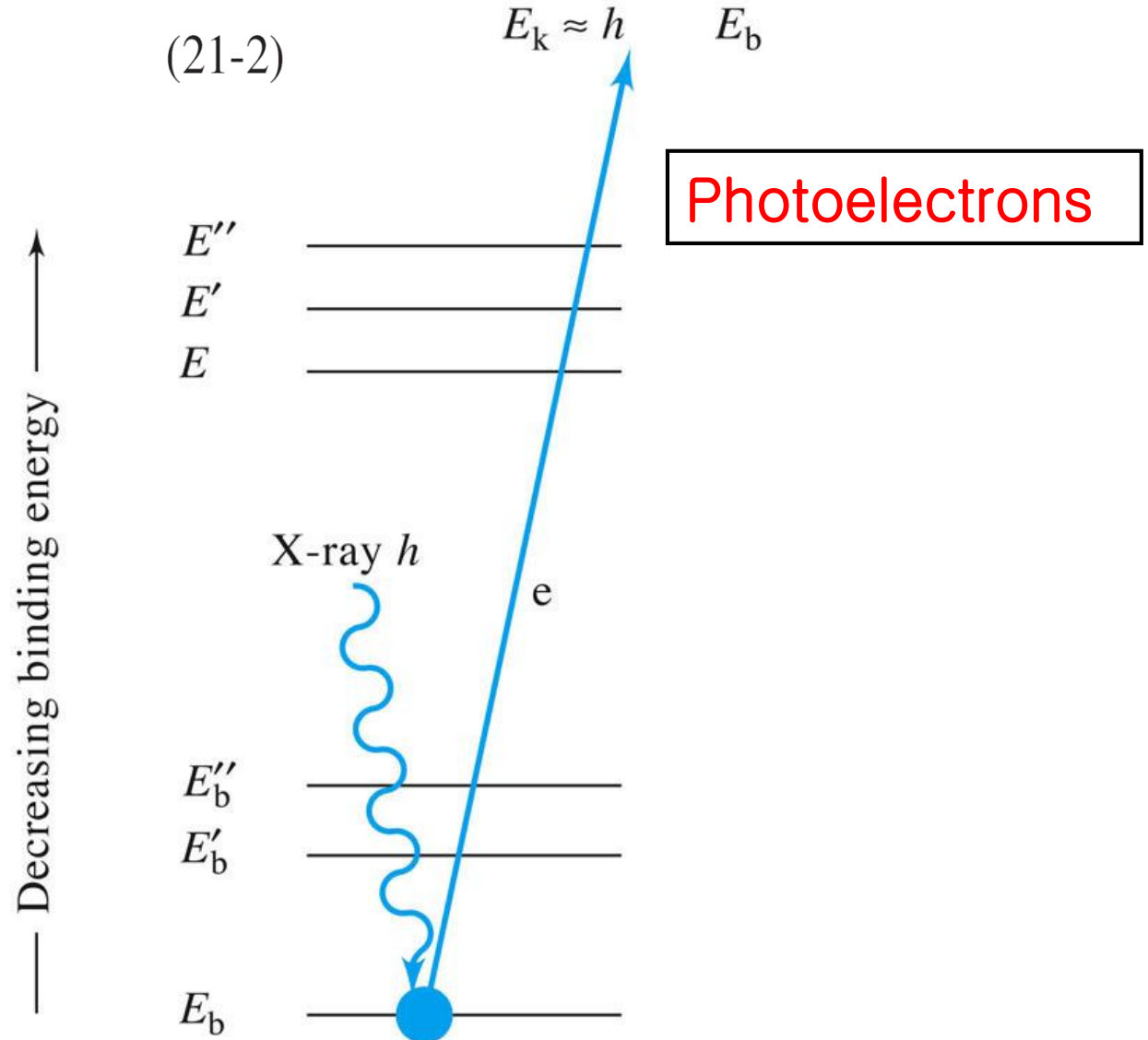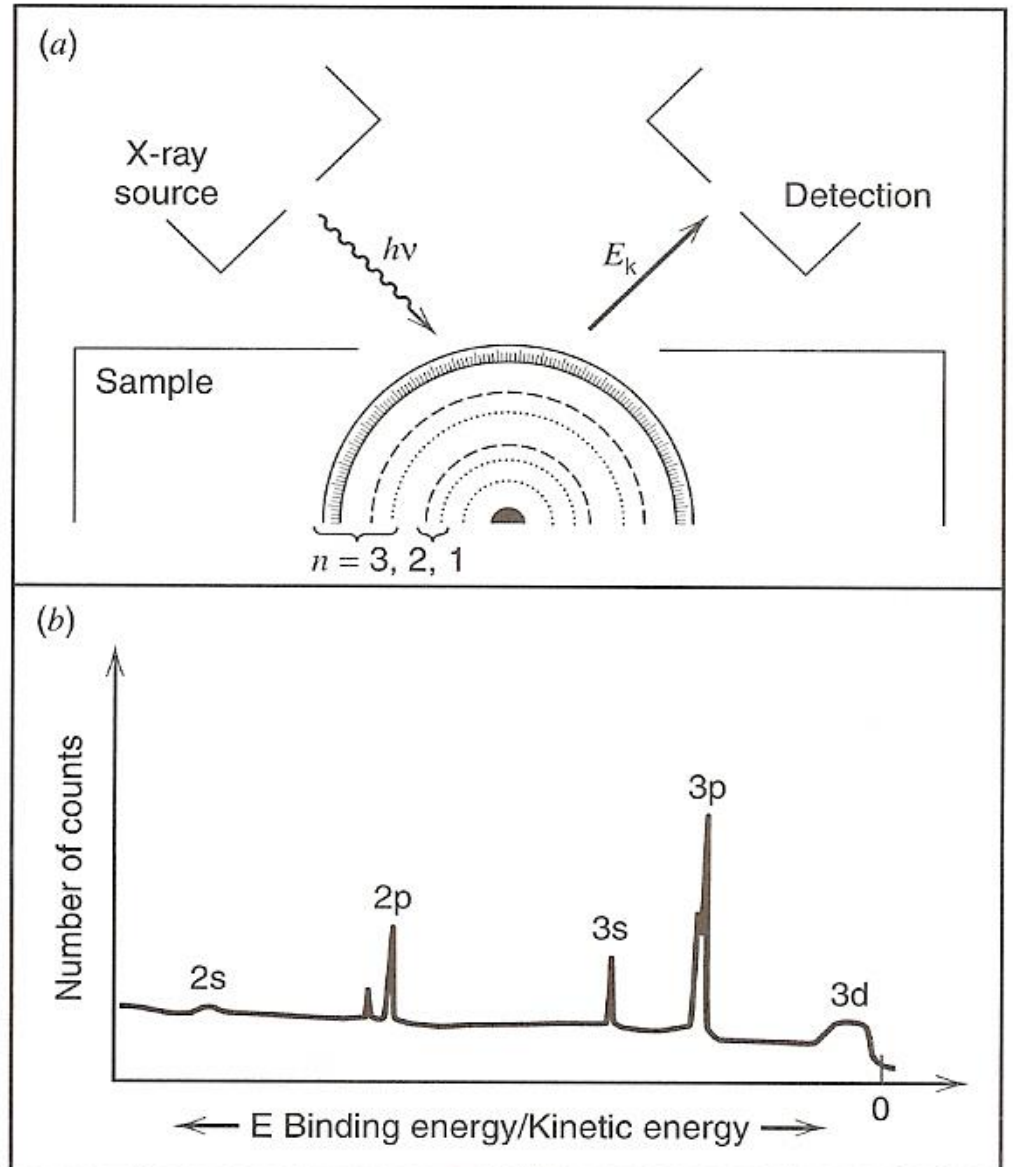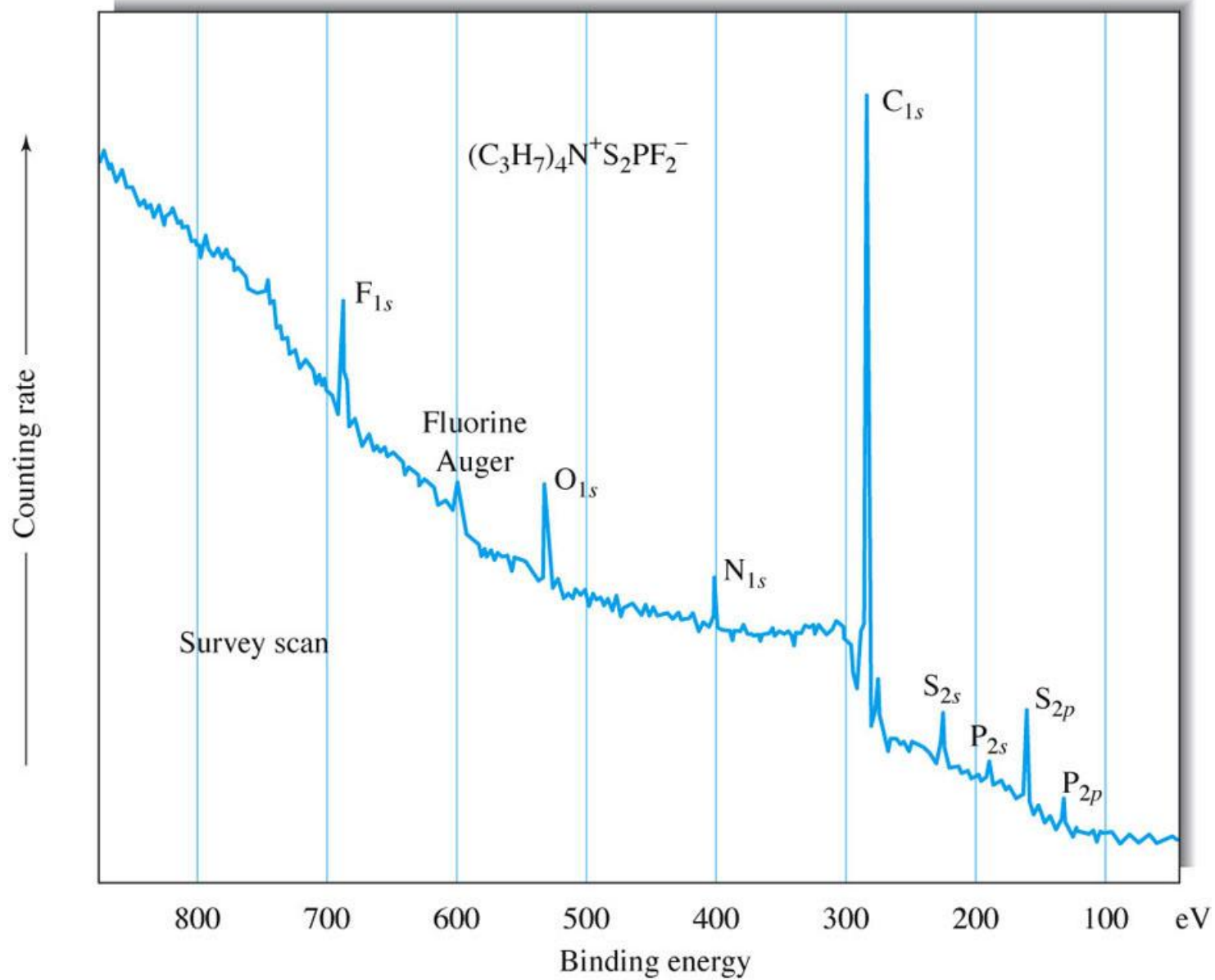
TABLE 21-2 Chemical Shifts as a Function of Oxidation State[a]

Element[b]	Oxidation State									
	−2	−1	0	+1	+2	+3	+4	+5	+6	+7
Nitrogen (1s)	—	*0[c]	—	+4.5[d]	—	+5.1	—	+8.0	—	—
Sulfur (1s)	−2.0	—	*0	—	—	—	+4.5	—	+5.8	—
Chlorine (2p)	—	*0	—	—	—	+3.8	—	+7.1	—	+9.5
Copper (1s)	—	—	*0	+0.7	+4.4	—	—	—	—	—
Iodine (4s)	—	*0	—	—	—	—	—	+5.3	—	+6.5
Europium (3d)	—	—	—	—	*0	+9.6	—	—	—	—

[a] All shifts are in electron volts measured relative to the oxidation states indicated by (*). (Reprinted with permission from D. M. Hercules, *Anal. Chem.*, **1970**, *42*, 28A. Copyright 1970 American Chemical Society.)

[b] Type of electrons given in parentheses.

[c] Arbitrary zero for measurement, end nitrogen in NaN_3.

[d] Middle nitrogen in NaN_3.

Oxidation state↑ → electron의 binding energy↑

Carbon 1s
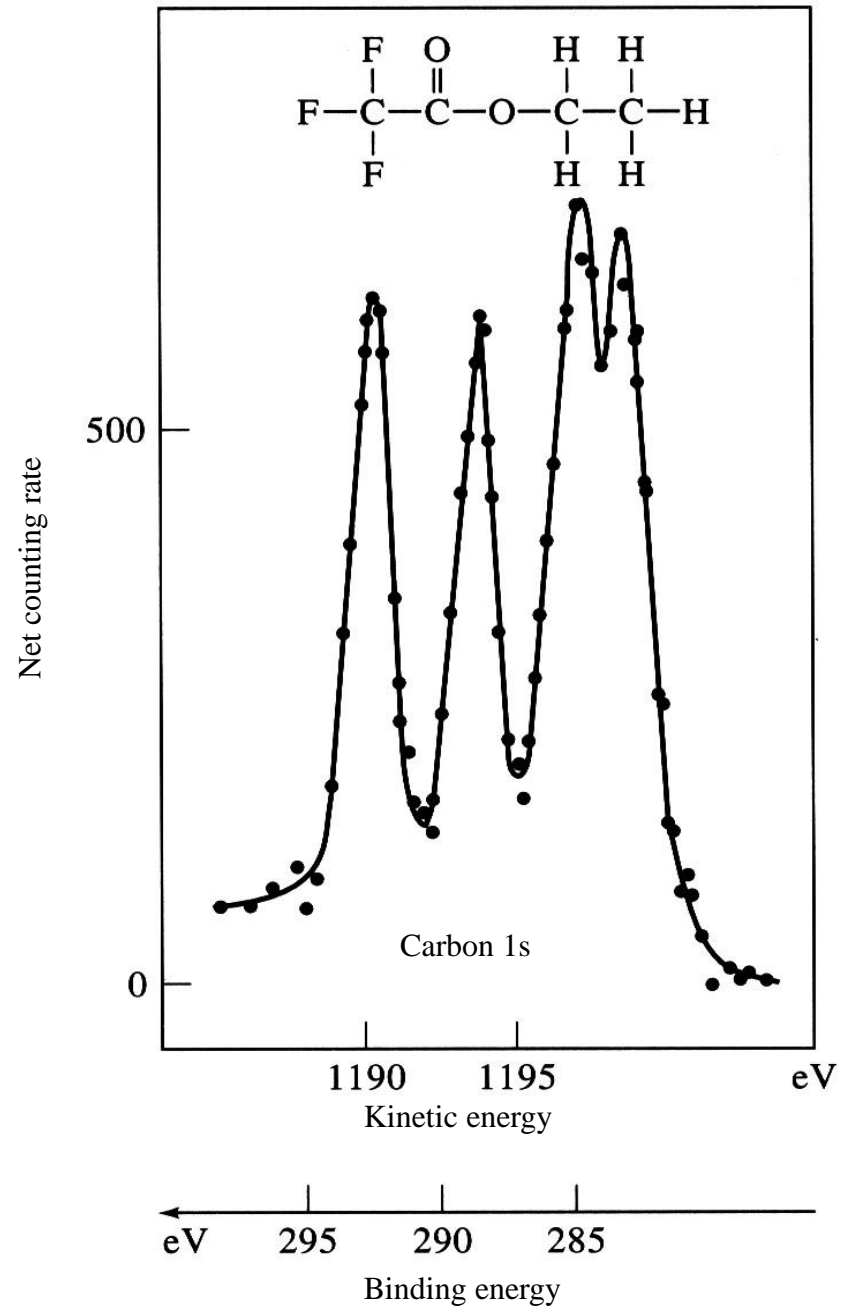
XPS quantitative analysis

$$I = n\phi\sigma\varepsilon\eta ATl \qquad (21\text{-}3)$$

Sensitivity factor

$$S = \sigma\varepsilon\eta ATl \qquad (21\text{-}4)$$

XPS for Pt 4f levels:
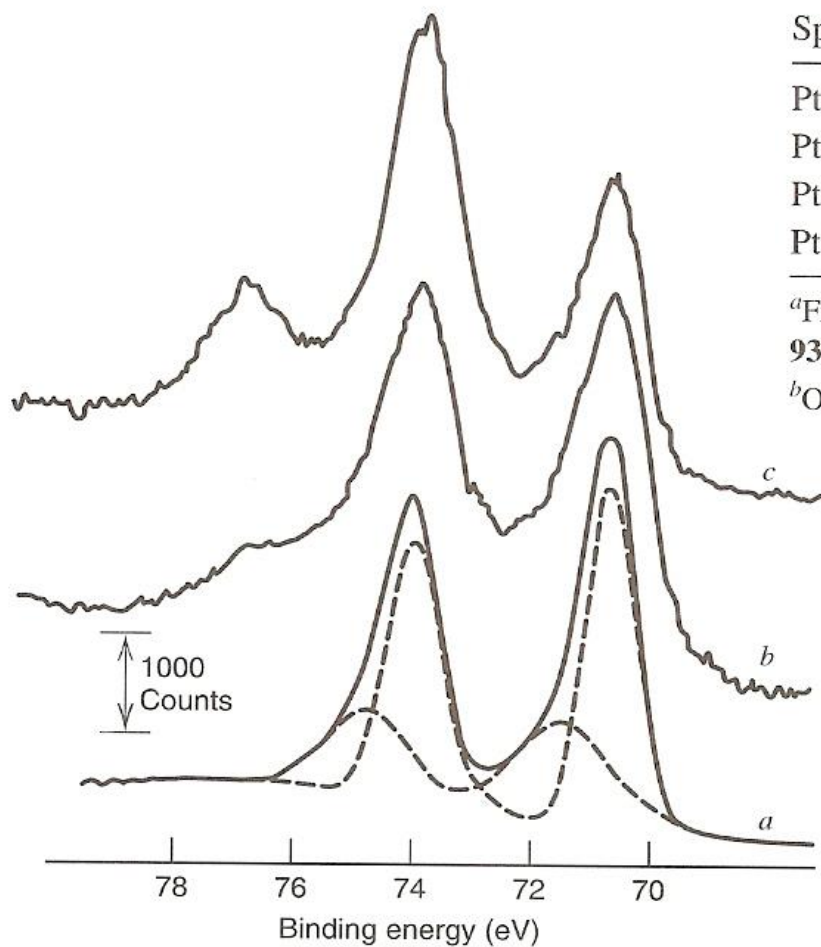
| Species | Binding Energy, eV | | Relative Peak Areas[b] | | |
	4f (7/2)	4f (5/2)	+0.7 V	+1.2 V	+2.2 V
Pt	70.7	74.0	56	39	34
PtO_{ads}	71.6	74.9	39	37	24
PtO	73.3	76.6	<5	24	22
PtO_2	74.1	77.4	0	0	20

[a]From K. S. Kim, N. Winograd, and R. E. Davis, *J. Am. Chem. Soc.*, **93**, 6296 (1971).

[b]Oxidation carried out at indicated potential (*vs.* SCE) for 3 min.

Electrochemical X-ray Photoelectron Spectroscopy

Univ. of Illinois

PtRu during Electrochemistry
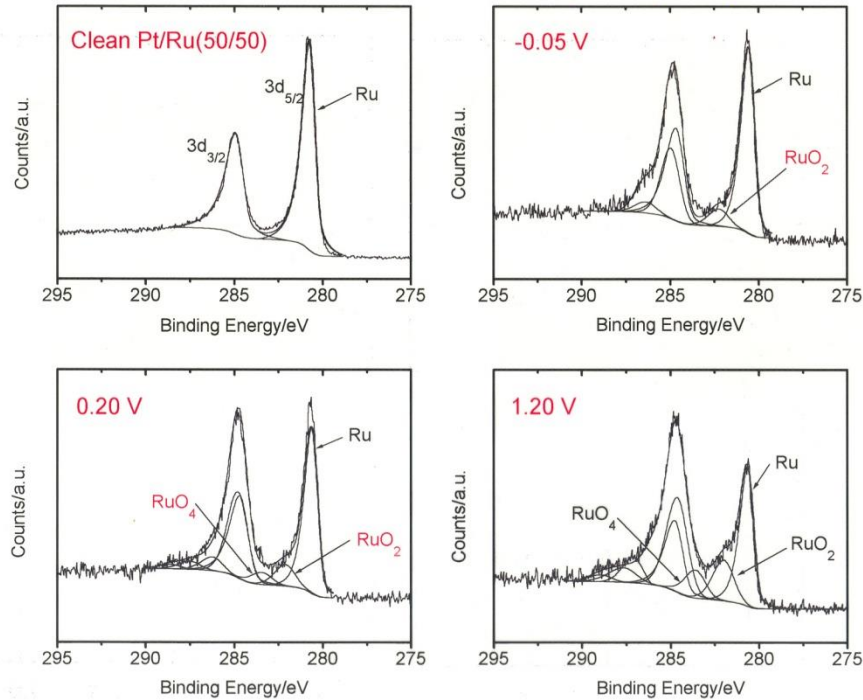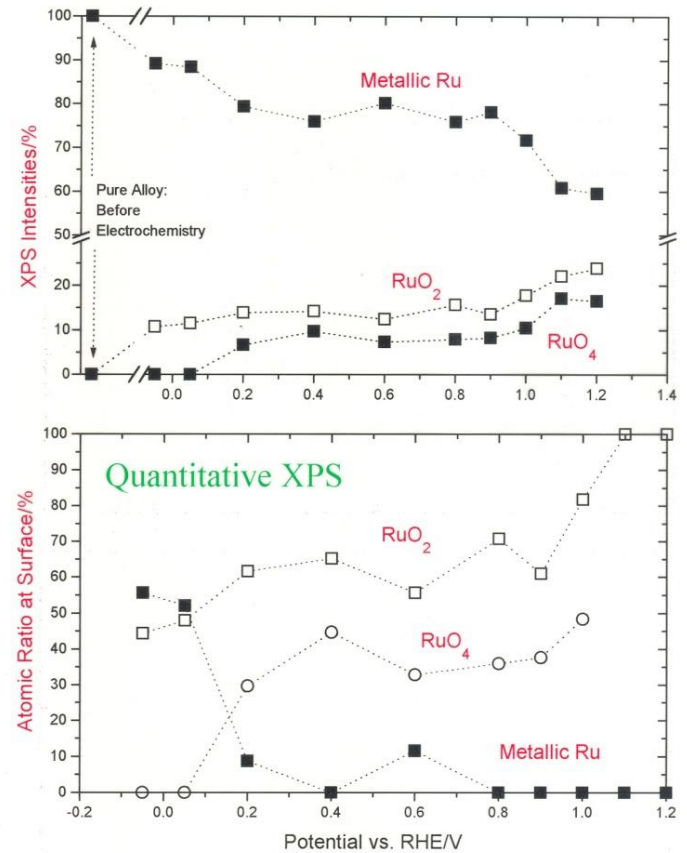
Electrochemical XPS (SNU)

UHV-XPS   **Glove Box**

Ex-situ Analysis without Contamination

Ambient Pressure X-ray Photoelectron Spectroscopy
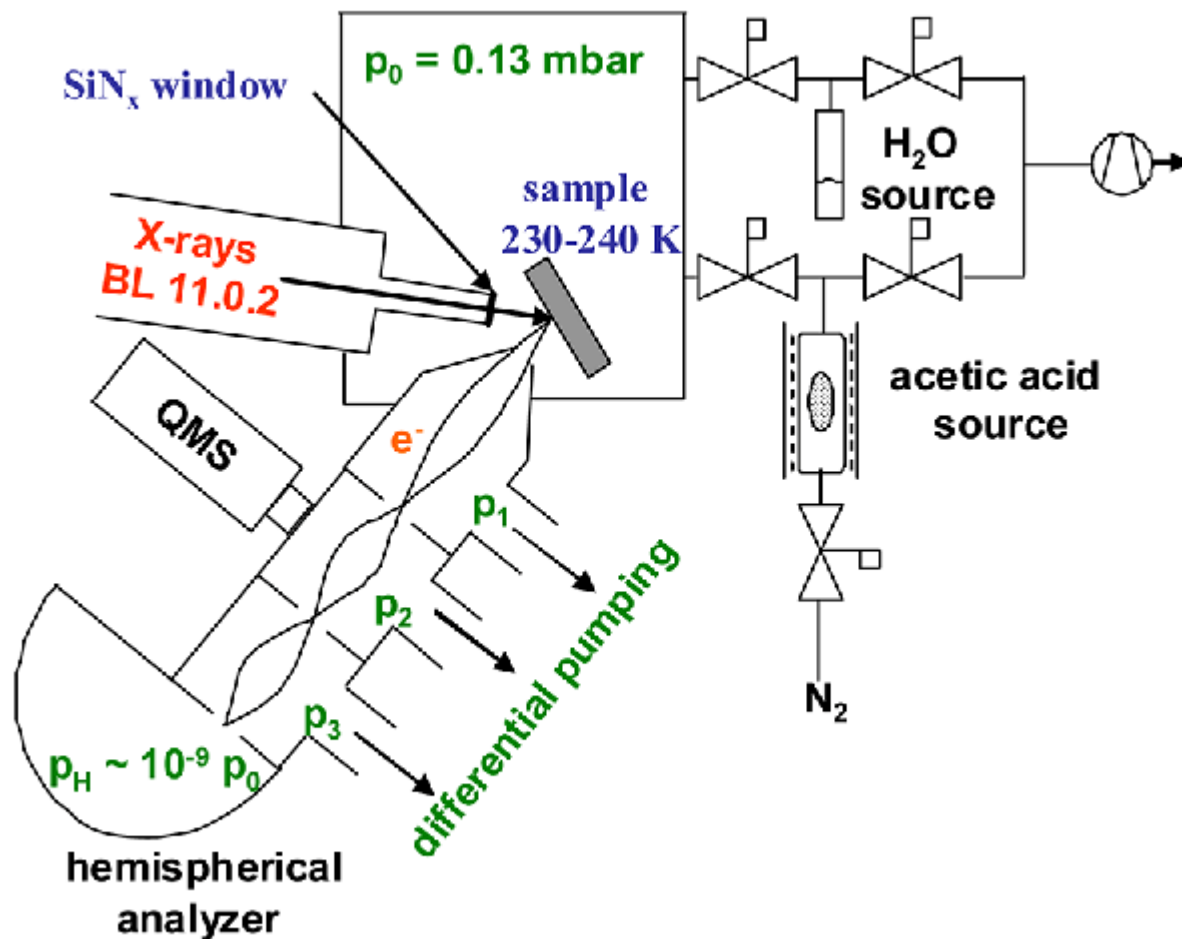
Ultraviolet photoelectron spectroscopy (UPS)

UV photons can excite photoemission from valence levels
Since valence electrons are involved in chemical bonding → UPS is well
suited to the study of bonding at surfaces → workfunction, band structure
of the solids, surface and adsorbed layers
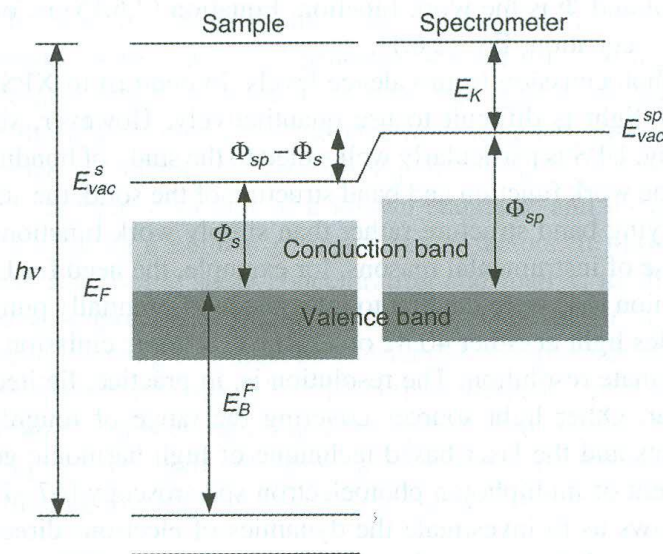
Figure 2.18 *The influence of the spectrometer work function, Φ_{sp}, on photoelectron spectra. Φ_s, work function of the sample; E_{vac}^{sp}, E_{vac}^{s}, vacuum energies of the spectrometer and the sample, respectively; E_F, Fermi energy; E_K, electron kinetic energy; E_B^F, binding energy; h, Planck constant; ν, frequency of incident photon. Adapted from J. C. Vickerman,* Surface Analysis: The Principal Techniques, *John Wiley, Chichester, Sussex. © 1997 with permission from John Wiley & Sons, Ltd.*
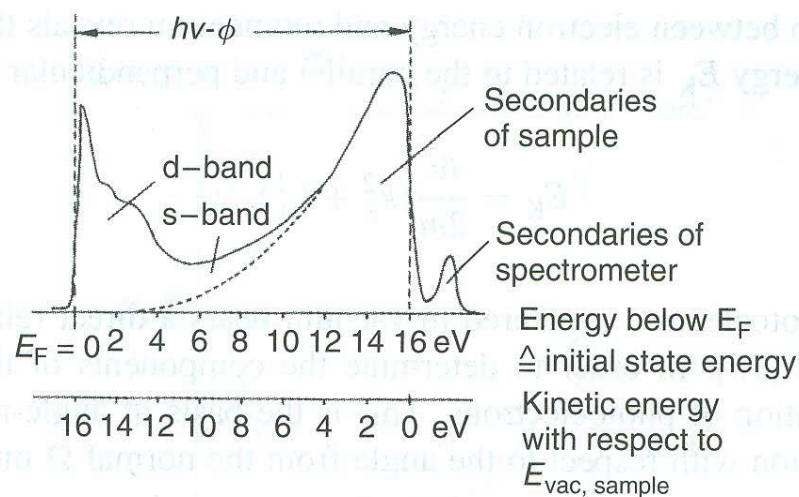
Figure 2.19 A representative ultraviolet photoelectron spectrum. The relative intensities of primary and secondary electrons depend on instrumental factors. E$_{vac}$, vacuum energy of the sample; E$_F$, Fermi energy; h, Planck constant; ν, frequency of the incident photon; Φ, sample work function. Reproduced from G. Ertl, J. Küppers, Low Energy Electrons and Surface Chemistry, 2nd ed., VCH, Weinheim. © 1985 with permission from John Wiley & Sons, Ltd.

Angle-resolved UPS (ARUPS)
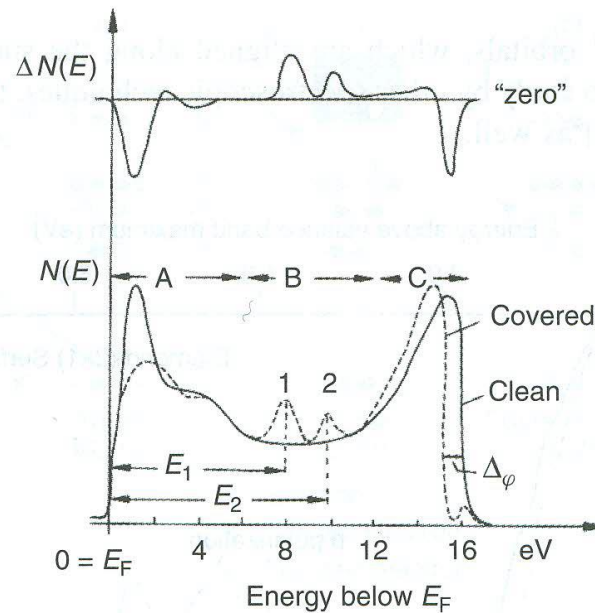
Figure 2.20 *Changes observed in ultraviolet photoemission spectra (lower panel) upon adsorption. The upper panel displays the difference spectrum.* $N(E)_{covered}$ *and* $N(E)_{clean}$ *are the count rates of photoelectrons from the adsorbate-covered and clean surface, respectively.* $\Delta N(E) = N(E)_{covered} - N(E)_{clean}$. *Reproduced from G. Ertl, J. Küppers, Low Energy Electrons and Surface Chemistry, 2nd ed., VCH, Weinheim.* © *1985 with permission from John Wiley & Sons, Ltd.*

Multiphoton photoemission (MPPE)
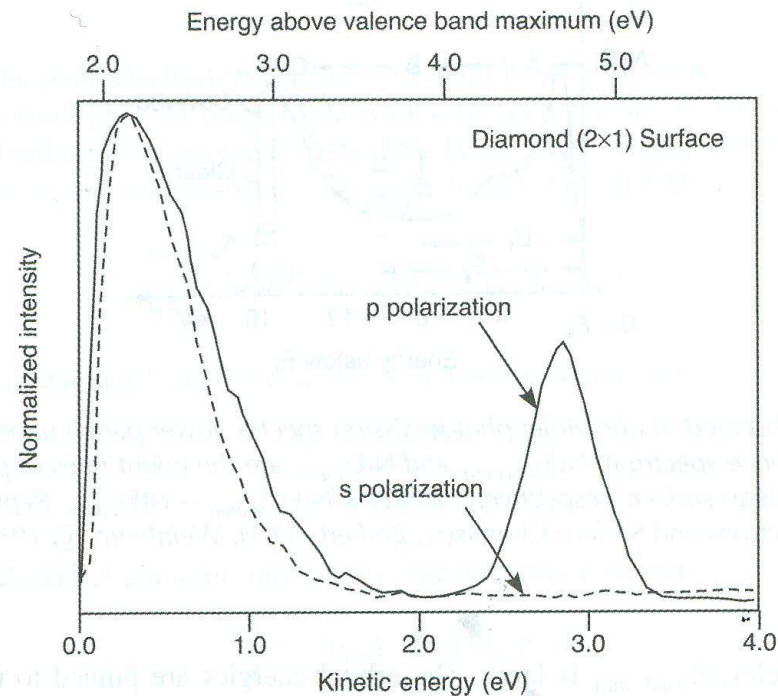
Figure 2.21 *Two-photon photoemission of the reconstructed C(111)–(2 × 1) diamond surface. The normally unoccupied surface state observed at ~3 eV is only observed with p-polarization due to selection rules. Reproduced from G.D. Kubiak, K.W. Kolasinski, Phys. Rev. B, 39, 1381. © 1989 with permission from the American Physical Society.*

Auger electron spectroscopy (AES)
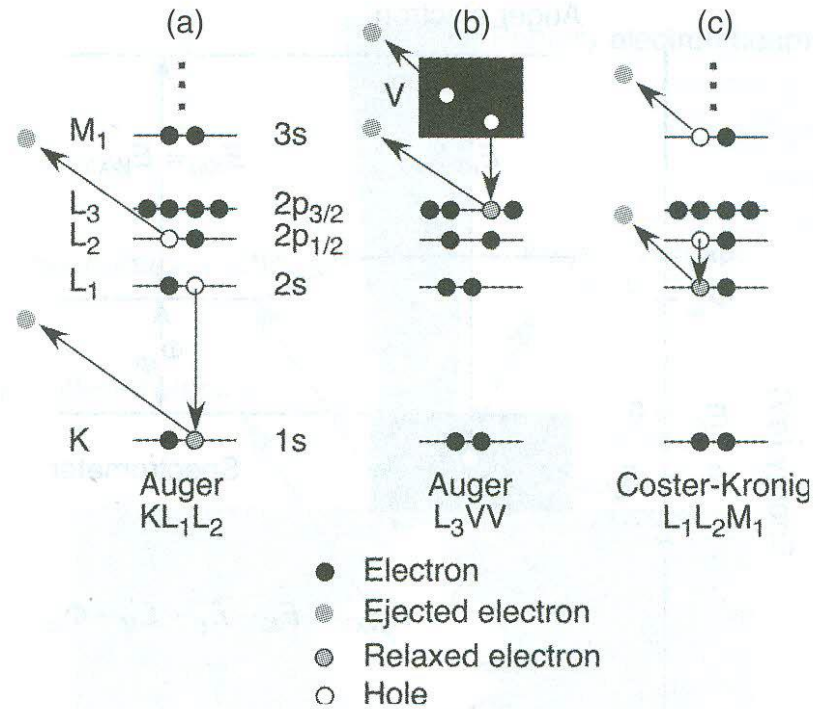
Figure 2.22 *A detailed depiction of Auger transitions involving (a) three core levels; (b) two core levels and the valence band; and (c) a Coster-Kronig transition in which the initial hole is filled from the same shell.*

Photoelectron Production

Auger Electron Production

M$_5$ — 3d$_{5/2}$

M$_4$ — 3d$_{3/2}$

M$_3$ — 3p$_{3/2}$

M$_2$ — 3p$_{1/2}$

M$_1$ — 3s$_{1/2}$

L$_3$ — 2p$_{3/2}$

L$_2$ — 2p$_{1/2}$

L$_1$ — 2s$_{1/2}$

$h\nu$

K or 1s Photoelectron

K — 1s$_{1/2}$

KL$_2$L$_3$ Auger Electron

$h\nu$
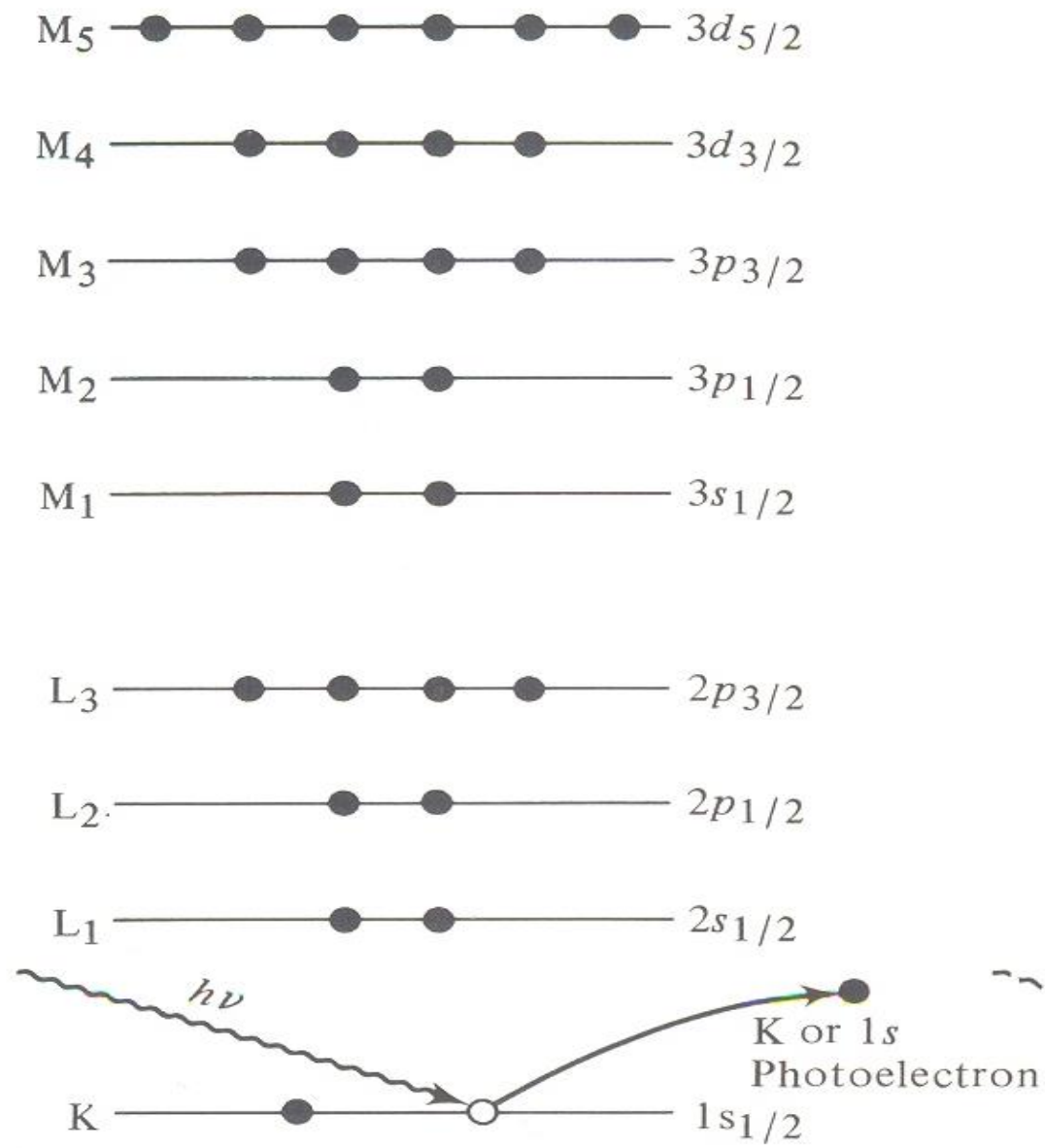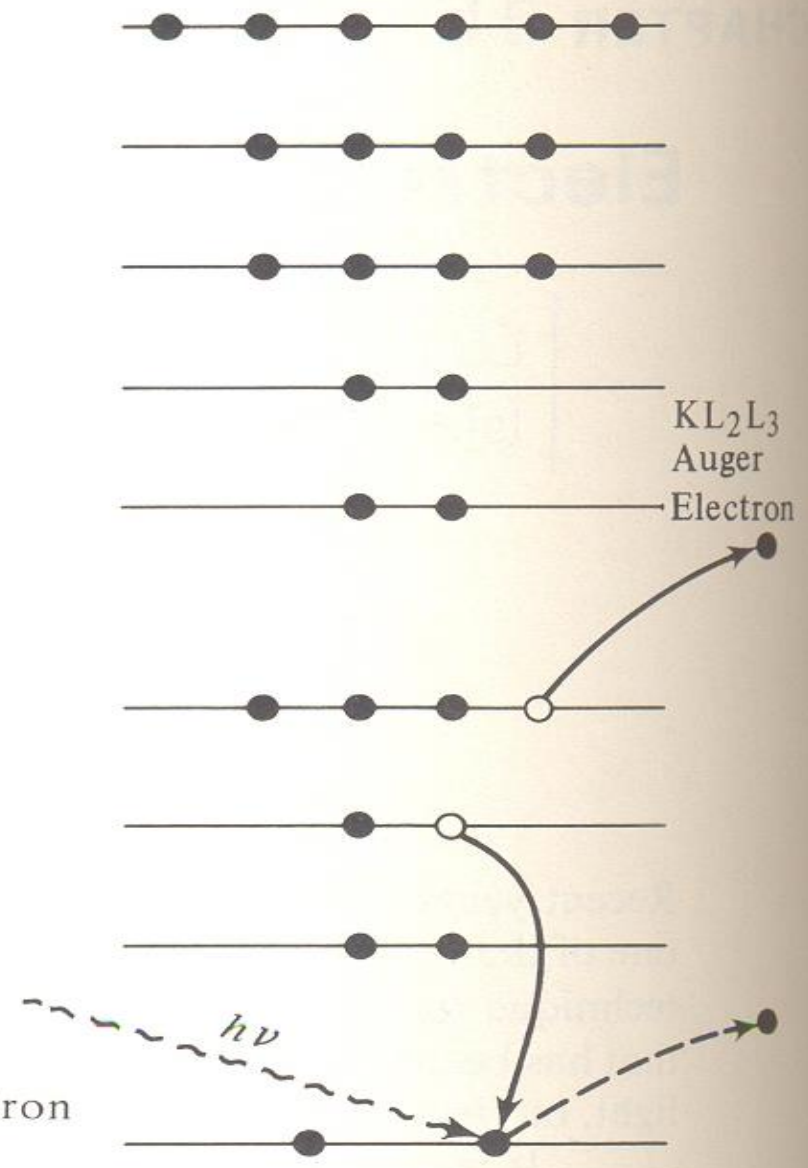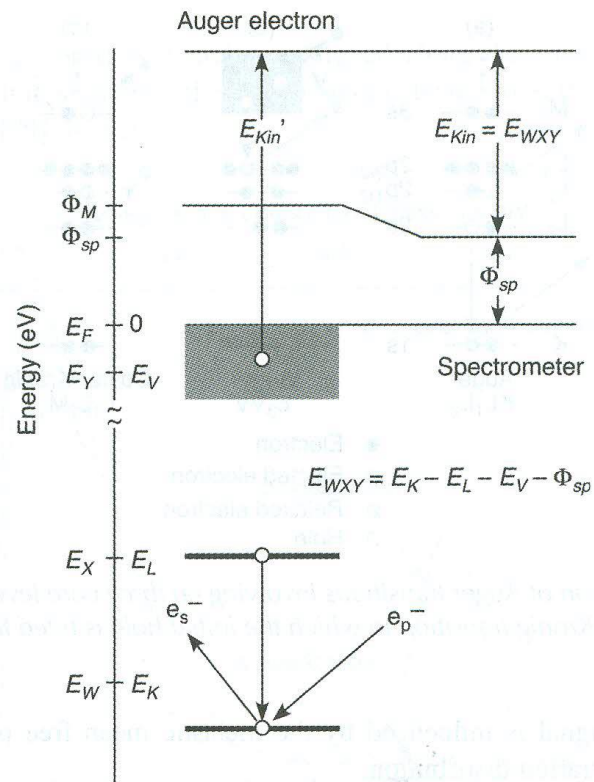
Figure 2.23 *Energy levels for a KLV Auger transition, including the influence of the spectrometer work function* Φ_{sp}. *Adapted from J.C. Vickerman,* Surface Analysis: The Principal Techniques, *John Wiley & Sons, Chichester.* © *1997 with permission from John Wiley & Sons, Ltd.*
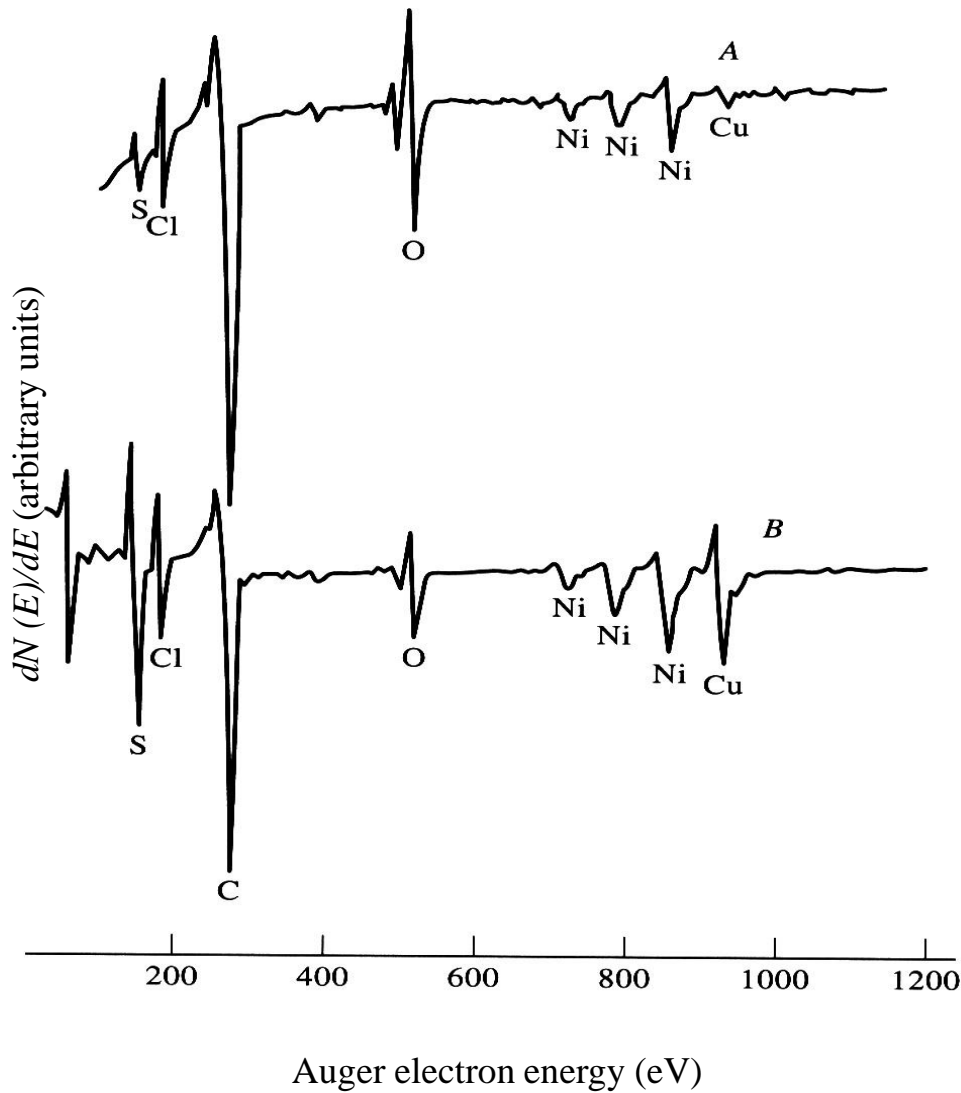
원소마다 고유한 Auger Electrons 방출

→ 원소 분석

Oxidation state

Structure

Quantitative analysis
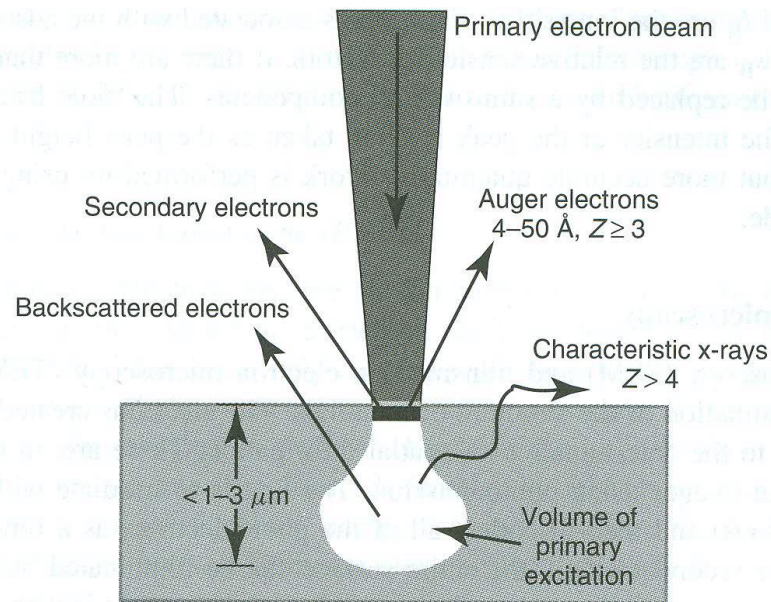
Figure 2.24 *The geometry of Auger electron spectroscopy. A primary electron beam excites the formation of Auger electrons as well as x-ray fluorescence. Backscattered and secondary electrons are also created in the process.*

AES depth profile: ion sputtering

Ion beam

Electron beam probe

Analyzed point

Etched crater

Specimen

© 2007 Thomson Higher Education
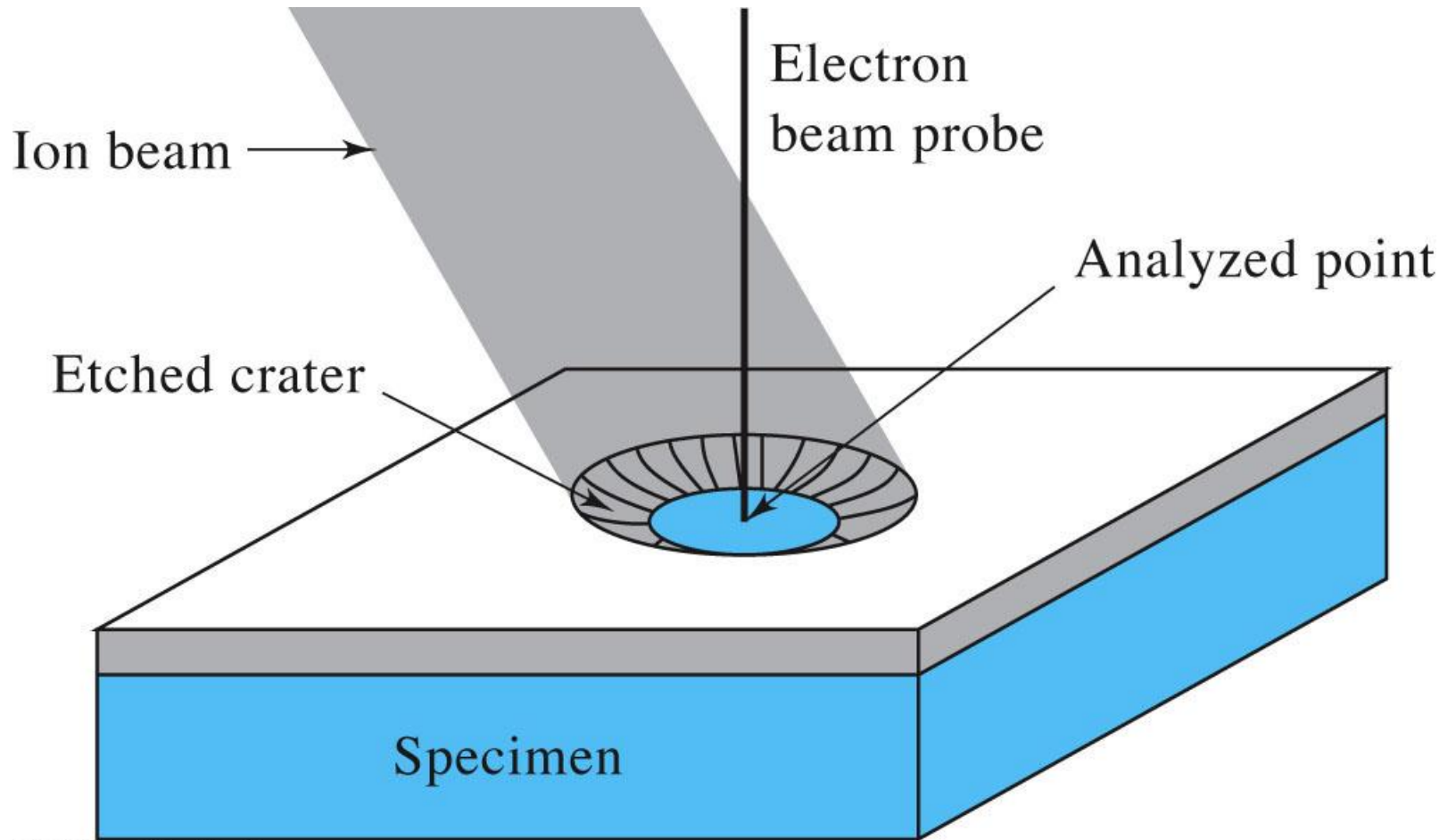
AES depth profiles: GaAs
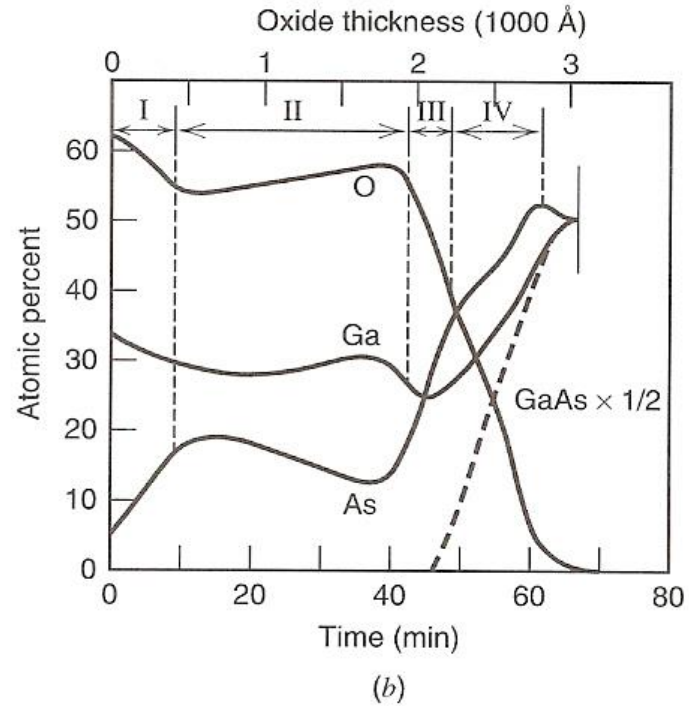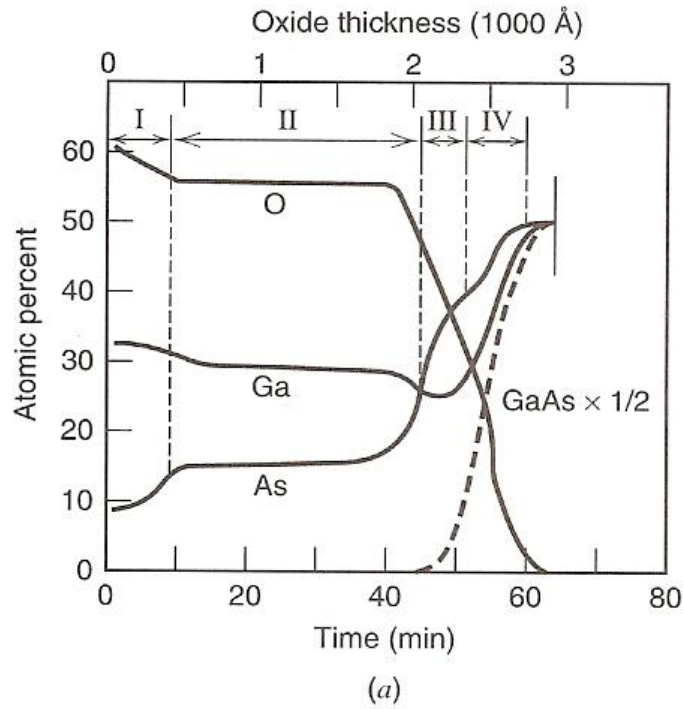
Electrochemical Auger Electron Spectroscopy

Univ. of Illinois
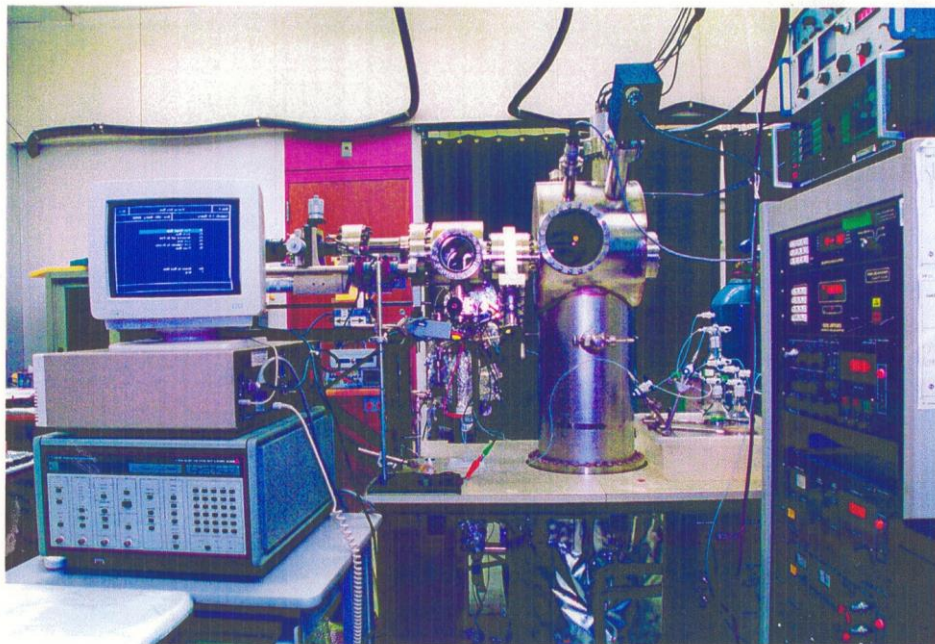
UHV-electrochemistry
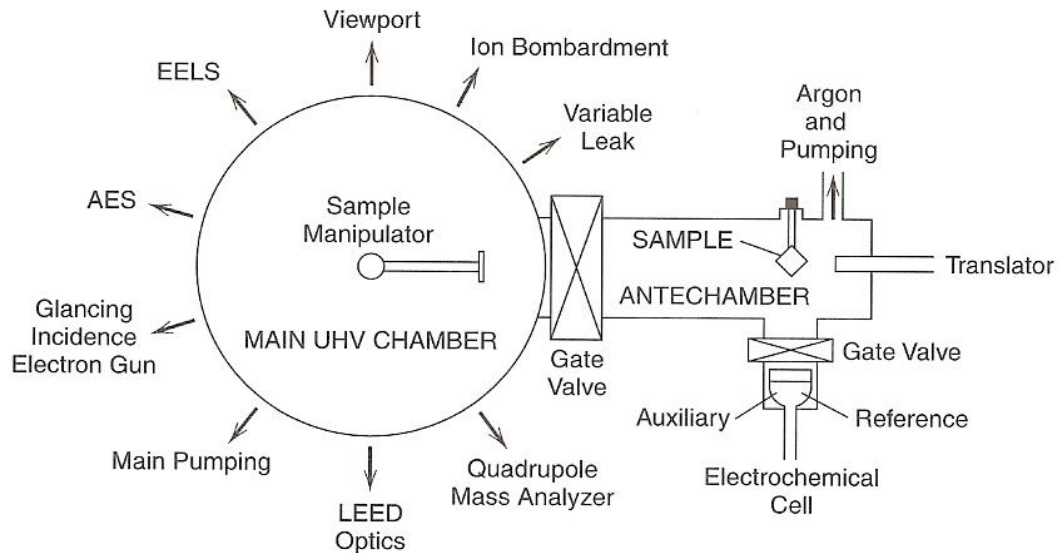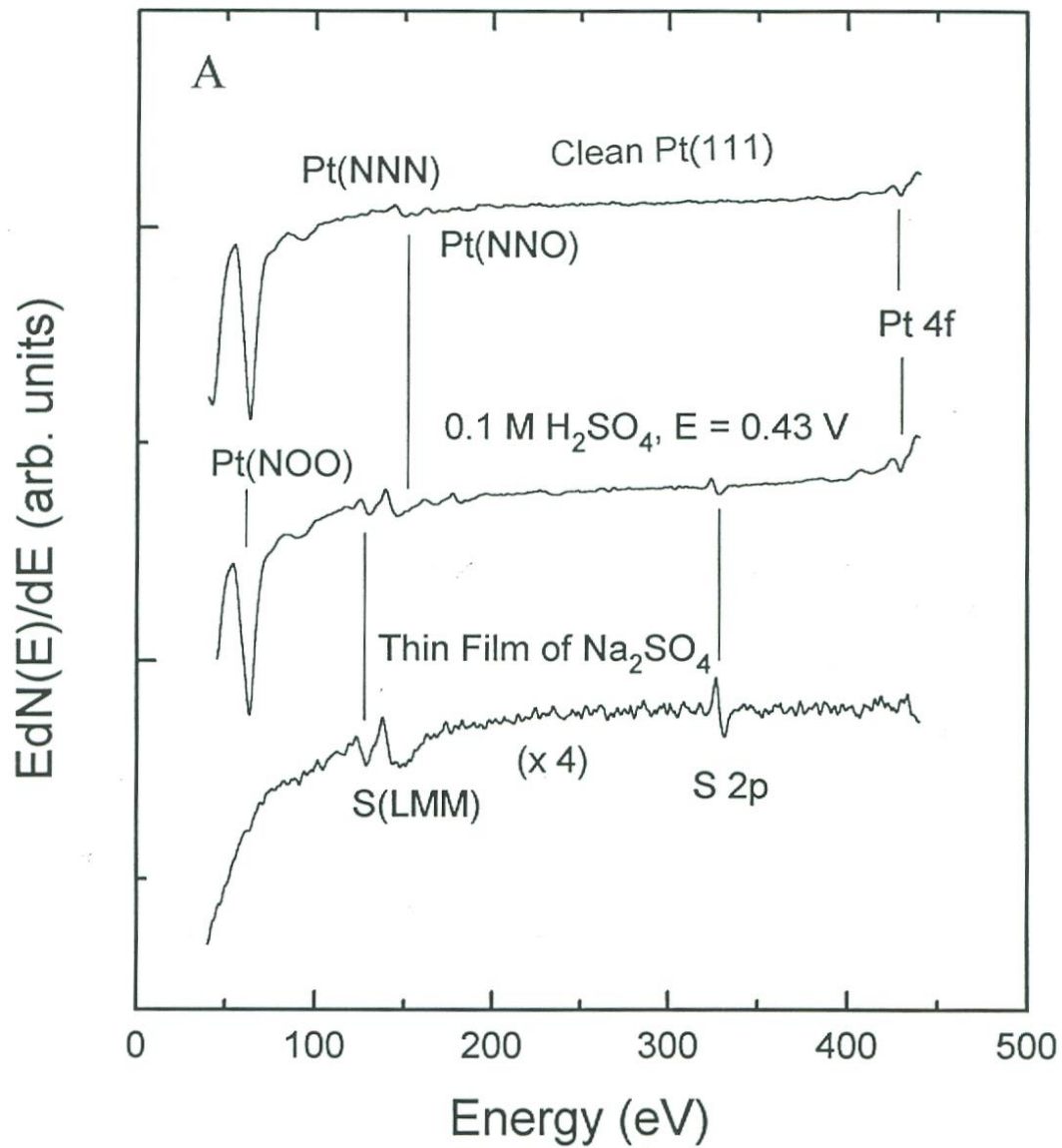
Quantitative Auger electron spectroscopy

$$\frac{I(S)}{I(S,0)} = \frac{r(S)}{r(S,0)} \cdot X \cdot \frac{\lambda(S)}{\lambda(S,0)} \cdot [\, 1 - \exp(-t\, /\, (\lambda(S)\cos\alpha))\,]$$

$$\frac{I(Ox)}{I(Ox,0)} = \frac{r(Ox)}{r(Ox,0)} \cdot Y \cdot \frac{\lambda(Ox)}{\lambda(Ox,0)} \cdot [\, 1 - \exp(-t\, /\, (\lambda(Ox)\cos\alpha))\,]$$

$$X = \frac{M(S)}{M(S,0)} \quad \text{for sulfur,} \quad Y = \frac{M(Ox)}{M(Ox,0)} \quad \text{for oxygen}$$

I: AES intensity (I(S): surface, I(S,0): bulk (from Na_2SO_4)
r: backscattering factor (계산 가능)
λ: inelastic mean free path (계산 가능)
t: overlayer thickness. α: electron escape angle(42.3° in CMA)

M(S,0): mean atomic density of sulfur in Na_2SO_4 (1/cm^3)

→ M(S) (mean atomic density of sulfur in the overlayer)

in situ (CV) vs. *ex situ* (LEED, AES)
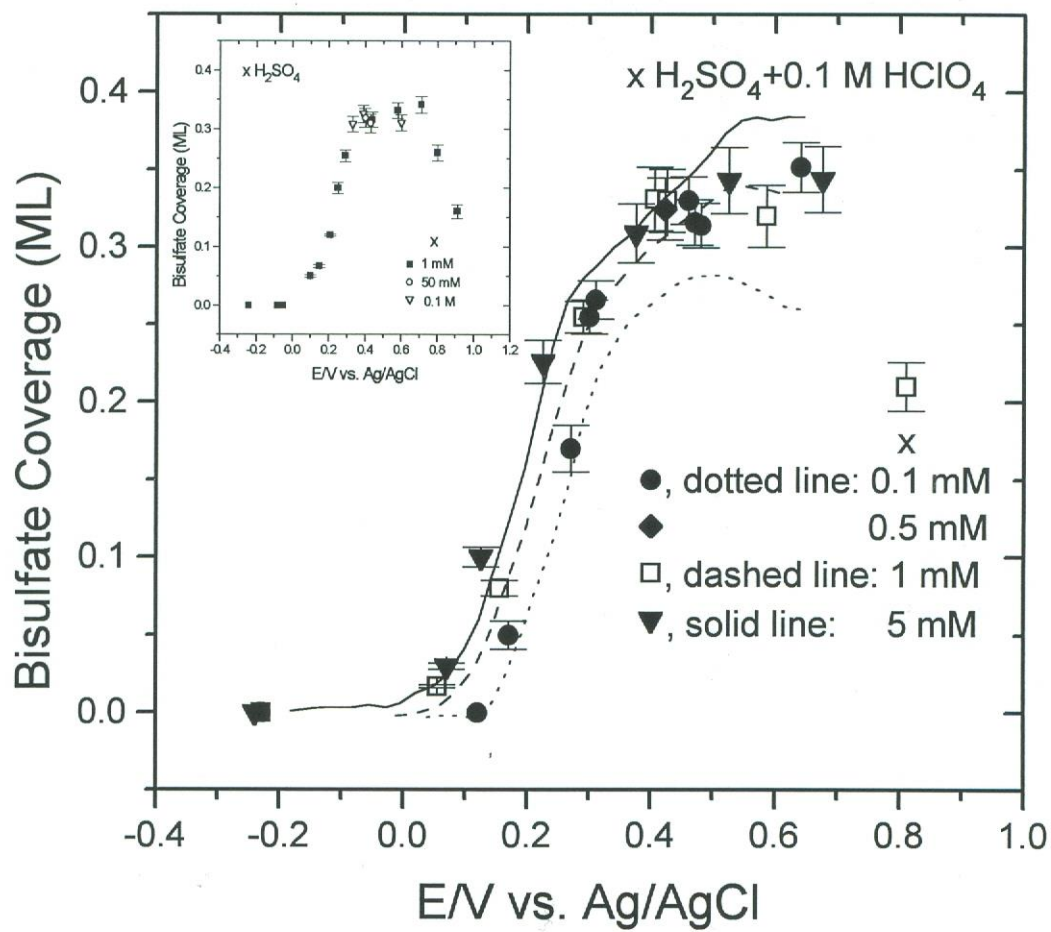
Vibration spectroscopy

Vibration motions → IR absorption, electron energy loss, Raman, sum frequency generation, inelastic neutron tunneling, He scattering

Energy of electromagnetic field: oscillating electric & magnetic disturbance

$$E = h\nu = h\,c/\lambda$$

h; Planck constant (6.6 x 10^{-34} Js)
speed of light (c); 3 x 10^8 m/s,
wavelength (λ); distance between the neighboring peaks of wave,
           1 Å = 0.1 nm = 10^{-10} m
frequency (ν, Hz = 1 s^{-1}); number of times per second
           $\lambda\nu = c$
wavenumber (cm^{-1}, reciprocal cm), ν-bar = ν/c = $1/\lambda$
cf) 1 eV ~ 8066 cm^{-1}

Wavelength (λ, nm) = 1240/band gap energy (eV)

Widely used IR spectroscopy: mid-IR ($670 \sim 4000$ cm^{-1}($2.5 \sim 14.9$ µm))

TABLE 17-1 Major Applications of IR Spectrometry

Spectral Regions	Measurement Type	Kind of Analysis	Applicable Samples
Near-IR	Diffuse reflectance	Quantitative	Solid or liquid commercial materials
	Absorption	Quantitative	Gaseous mixtures
Mid-IR	Absorption	Qualitative	Pure solid, liquid, or gases
		Quantitative	Complex liquid, solid, or gaseous mixtures
		Chromatographic	Complex liquid, solid, or gaseous mixtures
	Reflectance	Qualitative	Pure solids or liquids
	Emission	Quantitative	Atmospheric samples
Far-IR	Absorption	Qualitative	Pure inorganic or organometallic species

Electromagnetic spectrum
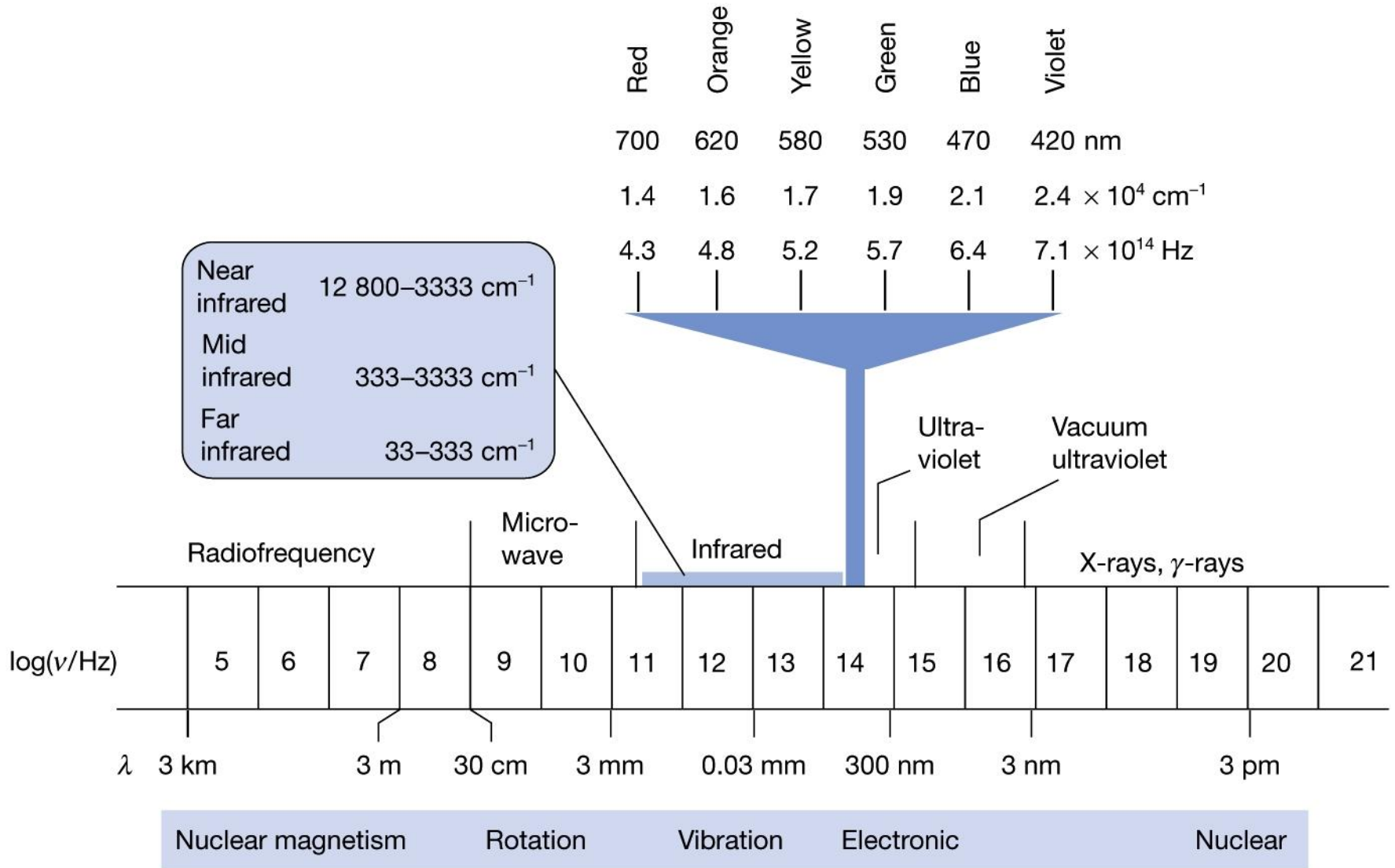
IR radiation ~ energy differences for vibrational & rotational states

For absorption of IR radiation: dipole moment change during vibration

Dipole moment is determined by the magnitude of the charge difference and the distance between two centers of charge
e.g) H-Cl (o)
     O-O   (x)

Types of vibration:
stretching & bending
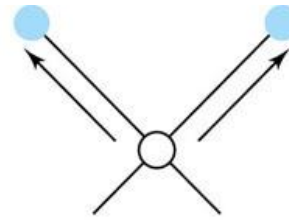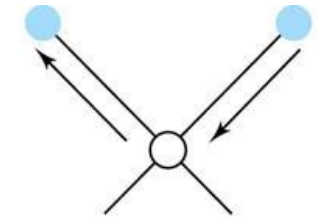
Symmetric   Asymmetric

(a) Stretching vibrations
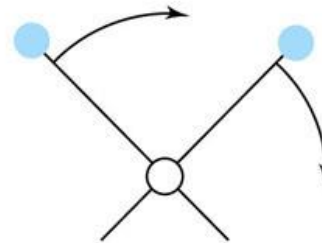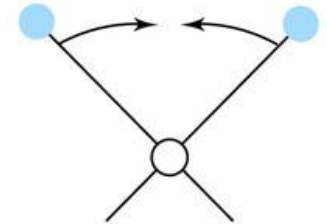
In-plane rocking   In-plane scissoring

+   +   +   −
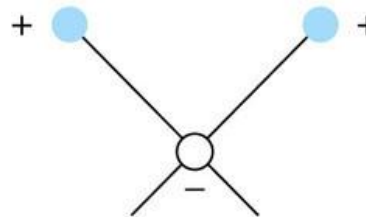
Out-of-plane wagging   Out-of-plane twisting
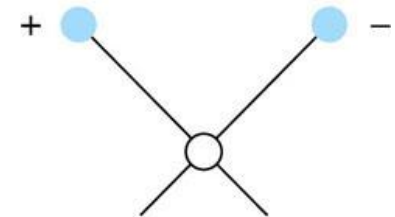
(b) Bending vibrations

© 2007 Thomson Higher Education

Harmonic oscillator

F = -ky   Hooke's law

k: force constant
-: opposite direction for the force

Potential energy:
$$E = \tfrac{1}{2}ky^2$$
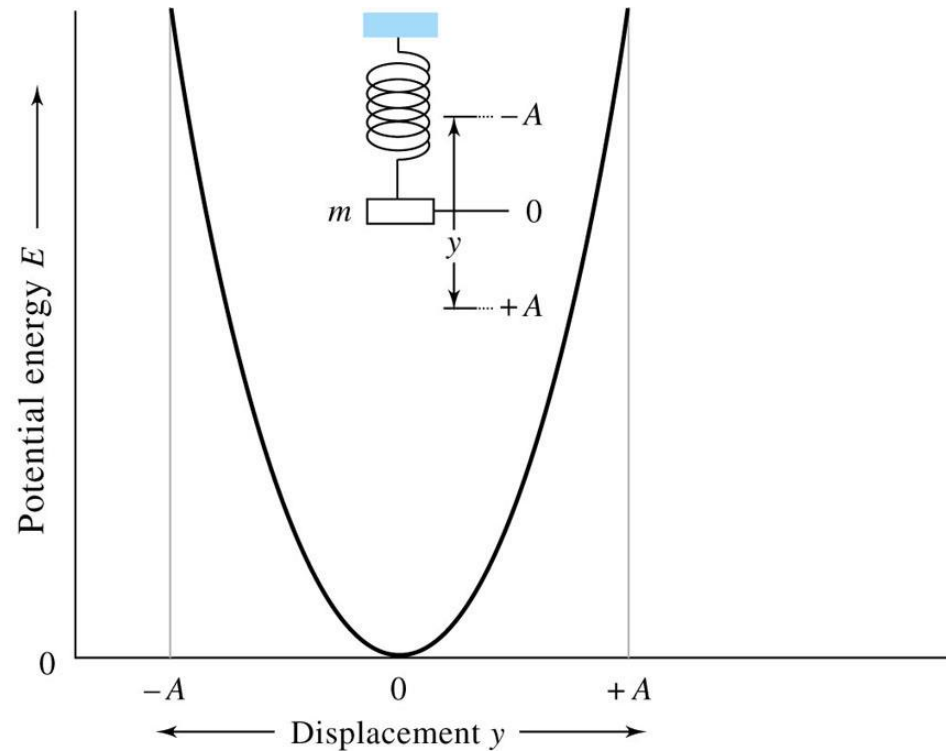
(a)

Vibrational frequency

$$F = ma = m(d^2y/dt^2) = -ky$$

$$y = A\cos(2\pi vt)$$

Frequency of mechanical oscillator

$$v = (1/2\pi)\sqrt{(k/m)}$$

Reduced mass: $\mu = m_1 m_2/(m_1 + m_2)$

$$v = (1/2\pi)\sqrt{(k/\mu)}$$

Quantum treatment of vibration:

$$E = (v + \tfrac{1}{2})(h/2\pi)\sqrt{(k/\mu)}$$

h: Planck's constant, v: vibrational quantum number

Transition v=0 to v=1

$\Delta E = h\nu = (h/2\pi)\sqrt{(k/\mu)}$

Ground state at v = 0:

$E_0 = \frac{1}{2} h\nu$

1st excited state (v= 1)

$E_1 = 3/2 h\nu$

Required radiation energy:

$(3/2 - \frac{1}{2})h\nu = h\nu$
$= (h/2\pi)\sqrt{(k/\mu)}$

Wavenumber (cm^{-1}):
v-bar $= (1/2\pi c)\sqrt{(k/\mu)}$
$= 5.3 \times 10^{-12}\sqrt{(k/\mu)}$

Dissociation energy

$v = 6$
$v = 5$
$v = 4$
$v = 3$
Energy level/
vibrational
quantum number
$v = 2$
$v = 1$
$v = 0$

Potential energy E

Interatomic distance r

(b)
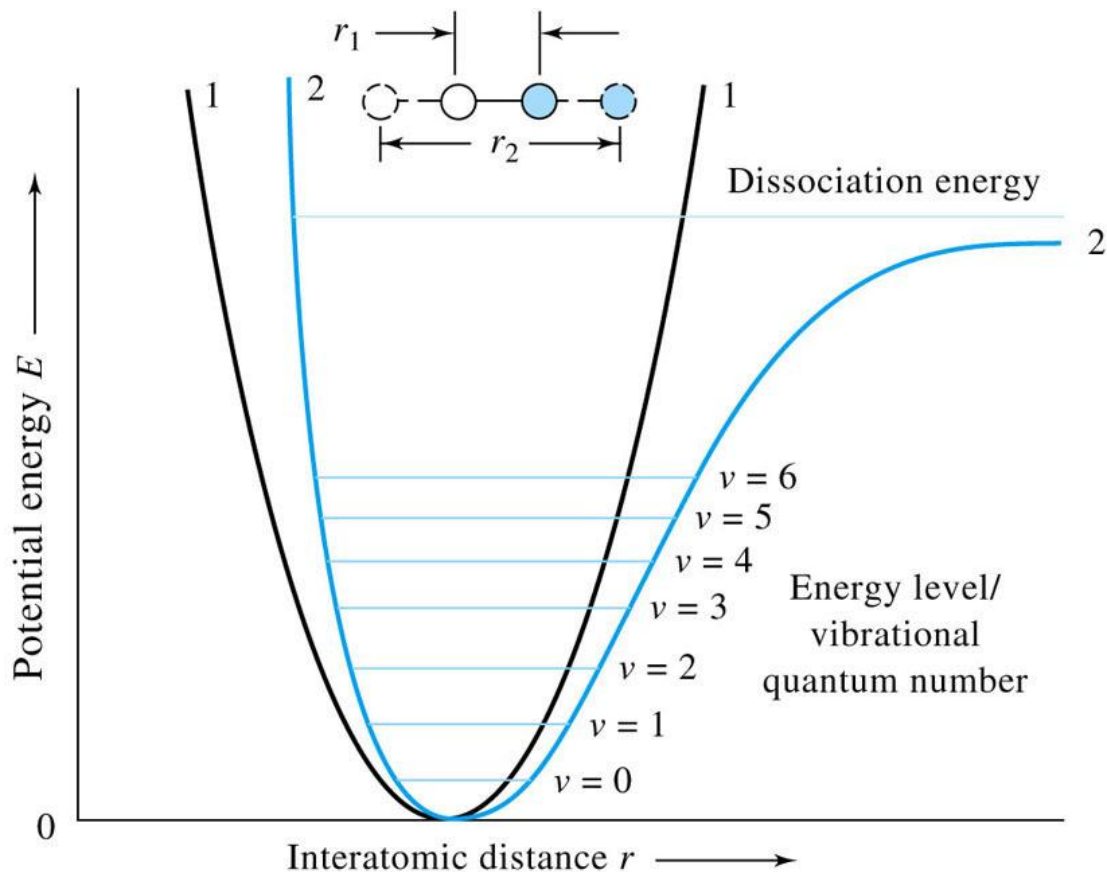
© 2007 Thomson Higher Education

1. Harmonic oscillator
2. Anharmonic motion

IR spectroscopy
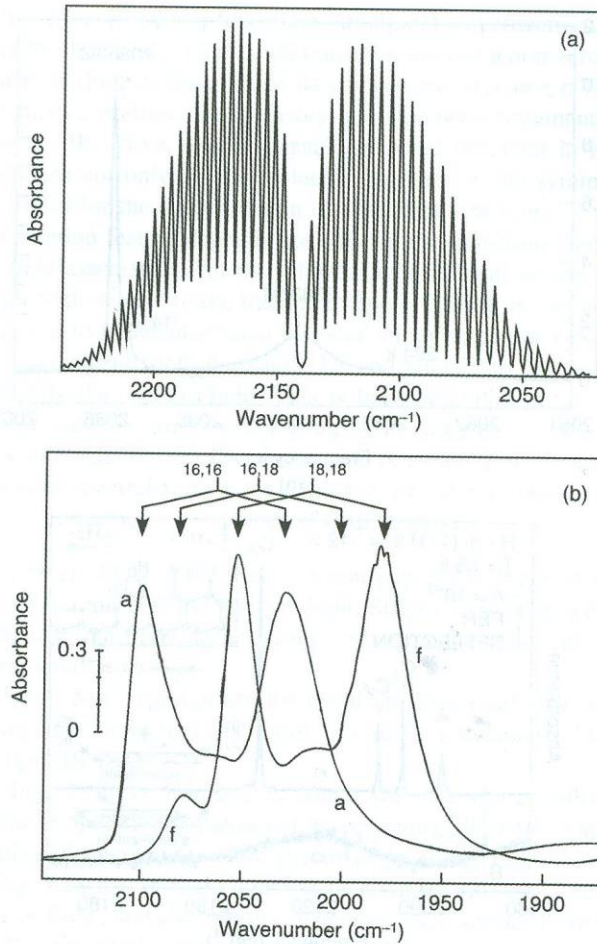
Figure 2.25 *The IR spectrum of (a) gas-phase CO versus that of (b) CO adsorbed on dispersed Rh clusters. The gas-phase spectrum exhibits rotational fine structure. The adsorbed CO forms a gem dicarbonyl species* $(Rh(CO)_2)$. *Coupling between the two adsorbed CO molecules leads to two vibrational peaks. The effect of oxygen isotopic substitution is also evident. 16,16 refers to* $Rh(C^{16}O)_2$, *etc. Adapted from J.T. Yates, Jr., K. Kolasinski, J. Chem. Phys., 79, 1026. © 1983 with permission from the American Institute of Physics.*
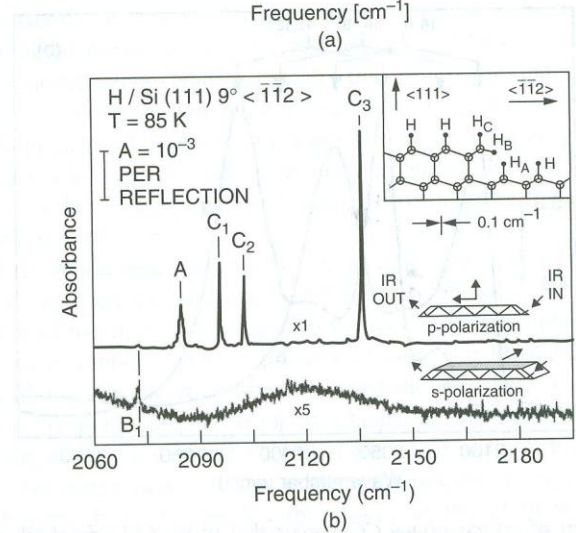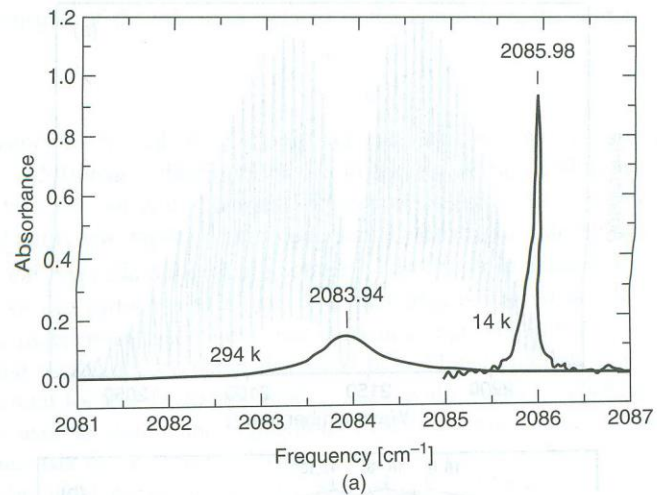
Figure 2.26 *The IR spectrum of H adsorbed on chemically prepared (a) flat and (b) stepped Si(111) surfaces. Part (a) reproduced from P. Jakob, Y.J. Chabal, K. Raghavachari,* Chem. Phys. Lett., *187, 325. (c) 1991 with permission from Elsevier. Part (b) reproduced from P. Jakob, Y.J. Chabal, K. Raghavachari, S.B. Christman,* Phys. Rev. B, *47, 6839. © 1993 with permission from the American Physical Society.*
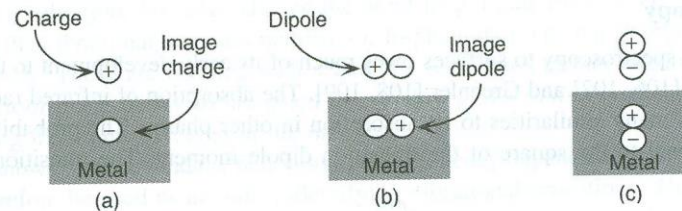

Figure 2.27 *Image dipole at a metallic surface.*

IR spectroscopy

Transmission
Reflection
Diffuse reflection
Internal reflection

I_0 I

(a)

(b)

(c)

(d)
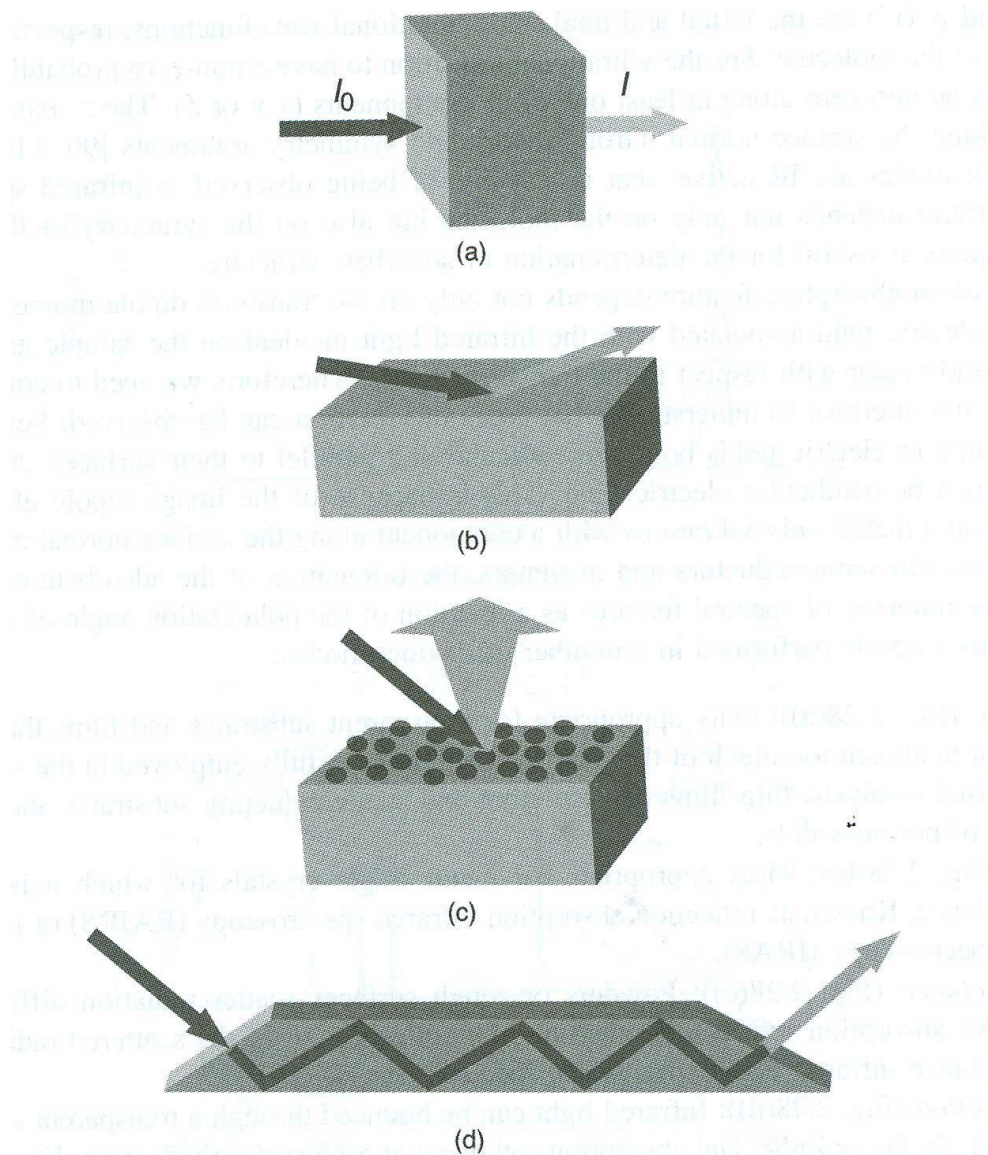
Figure 2.28 *The modes of IR spectroscopy.*

IR reflection spectroscopy

Specular reflection: smooth surface
Diffuse reflection
Internal reflection
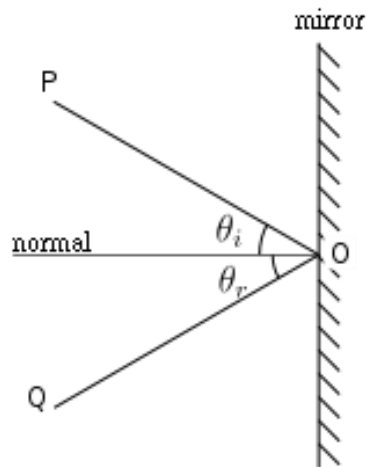
Specular reflection
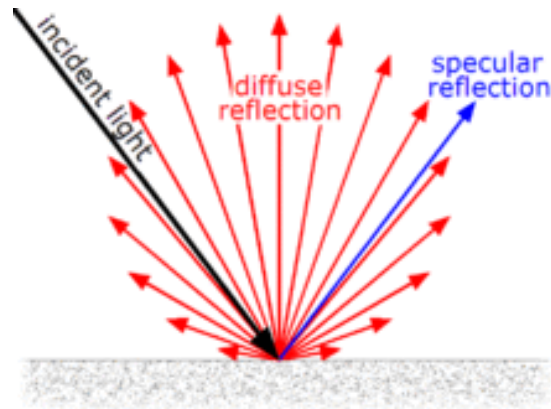
Diffuse reflection
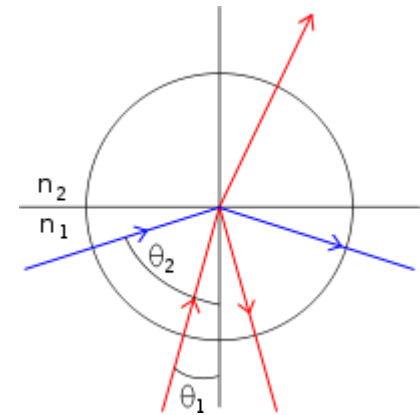
Internal reflection
(blue line)

Diffuse reflection

Diffuse-reflectance attachment

Ellipsoidal mirror

Sample cup

From interferometer

To detector

© 2007 Thomson Higher Education
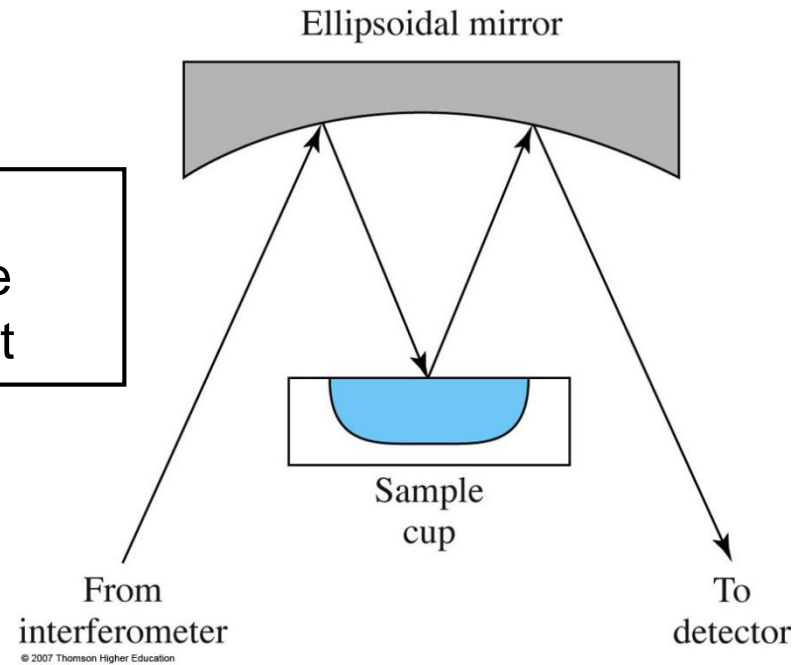
❖ Diffuse Reflectance Infrared Fourier Transform Spectroscopy (DRIFT)

IR beam

IR source

sample

detector
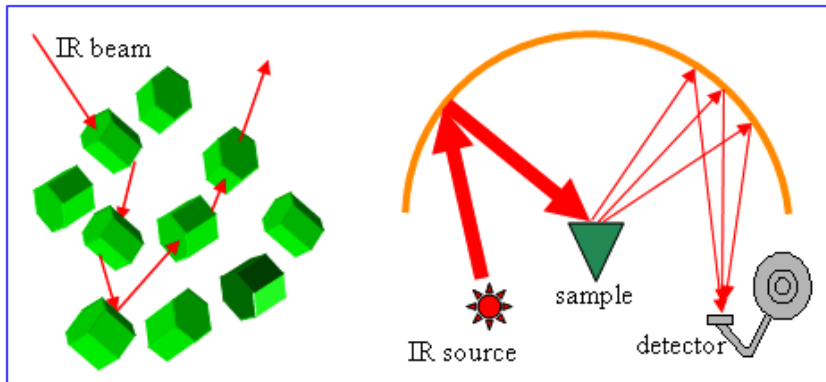
Powder sample

Electron energy loss spectroscopy (EELS)
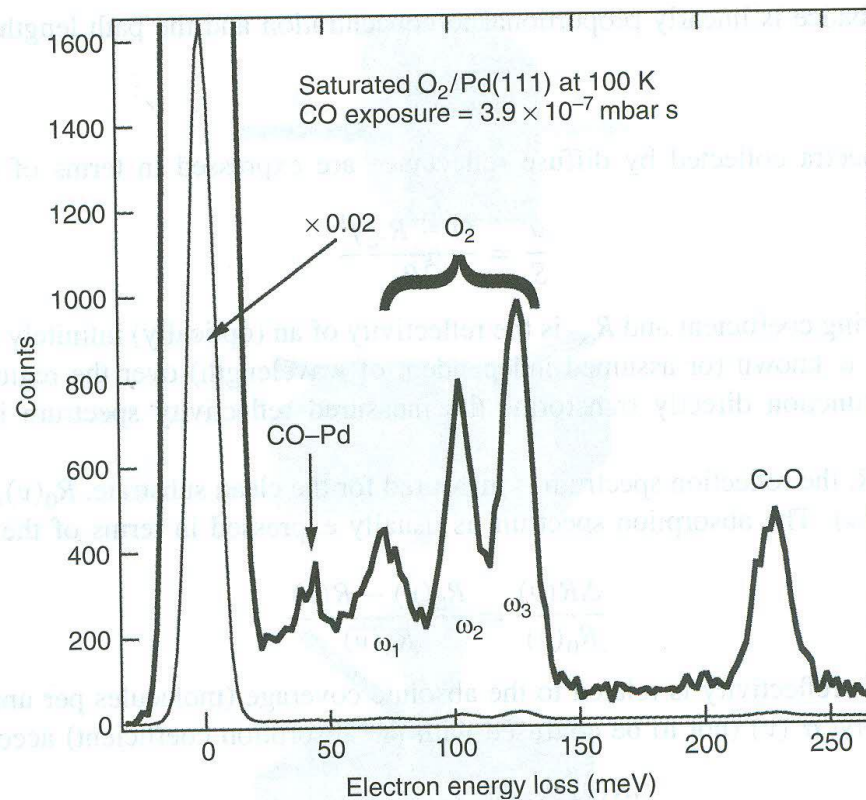
Figure 2.29 *The electron energy loss spectrum of co-adsorbed O_2 + CO on Pd(111). The species associated with ω_1, ω_2 and ω_3 are illustrated in Fig. 3.8. Adapted from K.W. Kolasinski, F. Cemič, A. de Meijere, E. Hasselbrink, Surf. Sci., 334, 19. © 1995 with permission from Elsevier.*

High resolution electron energy loss spectroscopy
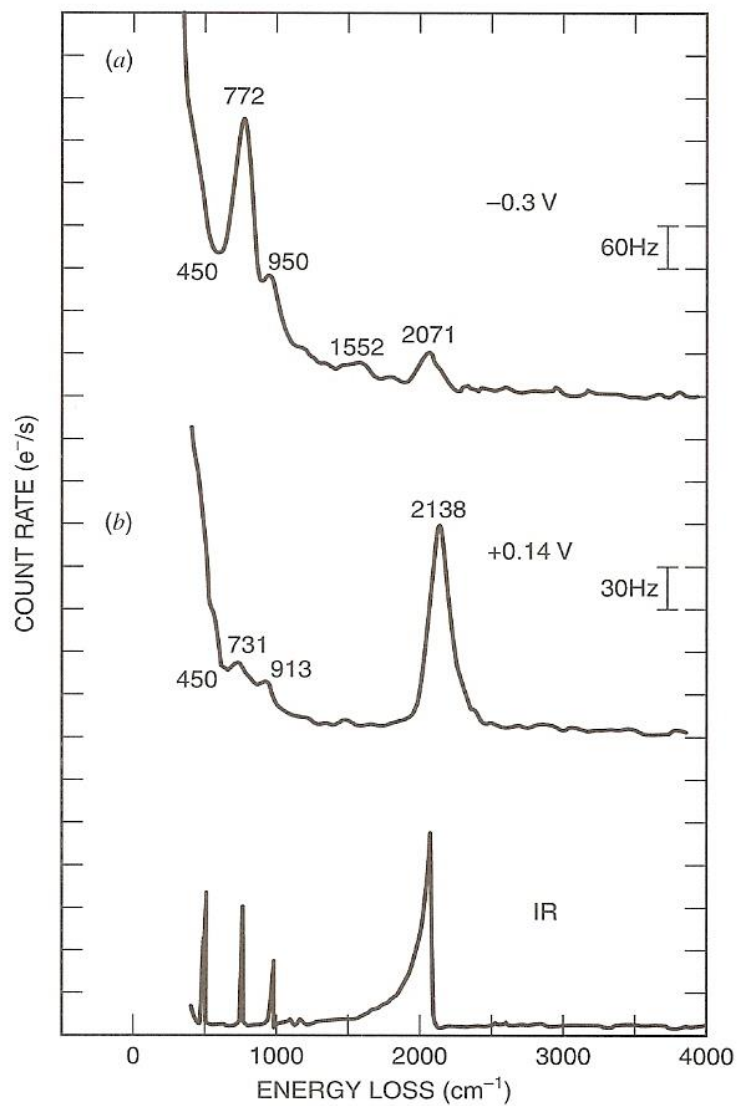
SCN$^-$ on Ag(111)

(a) -0.3 V
(b) +0.14 V

Second harmonic and sum frequency generation
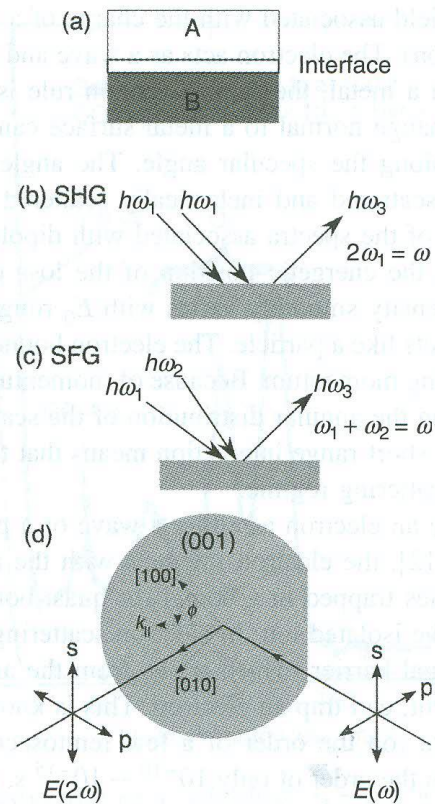
Figure 2.30 (a) Two bulk materials joined by an interfacial region. (b) Two photons of the same frequency are mixed in second harmonic generation (SHG). (c) Two photons of different frequency are mixed in sum frequency generation (SFG). (d) The polarization components s and p are shown for a laser incident on a surface.

Second harmonic spectroscopy

Second harmonic generation (SHG): $\omega \rightarrow 2\omega$
Second harmonic generation (SHG): noncentrosymmetric crystals
If symmetry is broken at the solid/liquid interface $\rightarrow$ SHG signal

SHG signal is sensitive to species at the interface: used to detect
adsorbed species, reaction intermediates etc
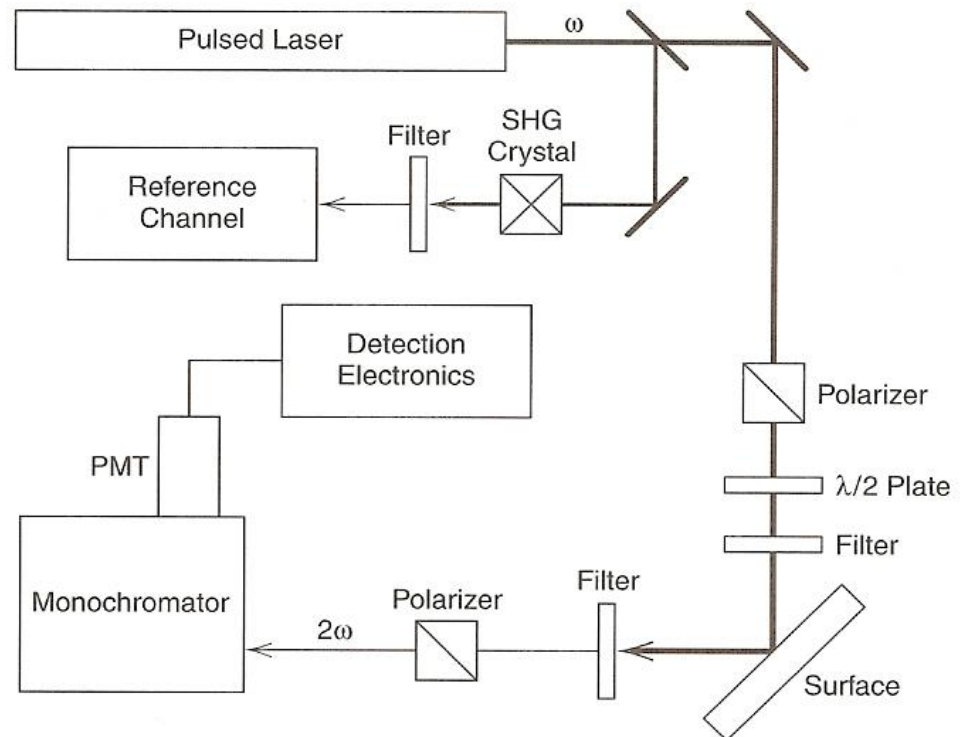
SHG response
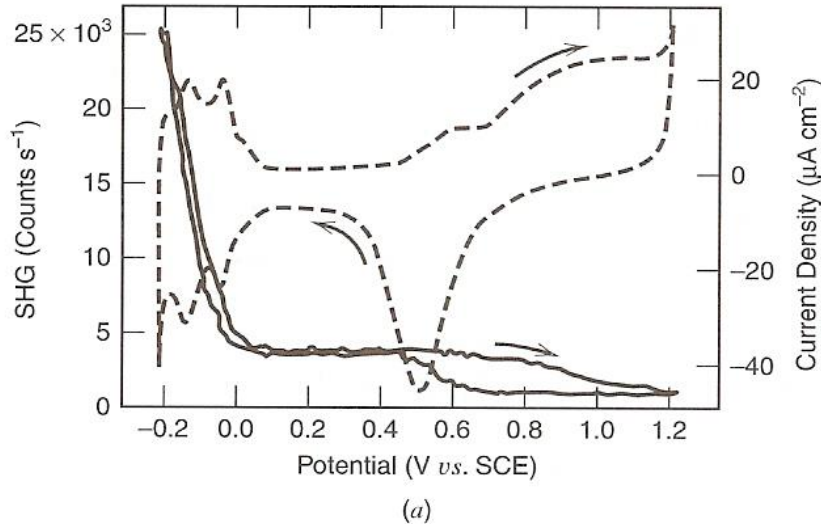
Polycrystalline Pt in $HClO_4$/KCl
CV vs. SHG signal

Neg. potential: adsorbed
    hydrogen
0~0.4 V: adsorbed chloride ion
>0.4 V: oxide or adsorbed
    hydroxyl
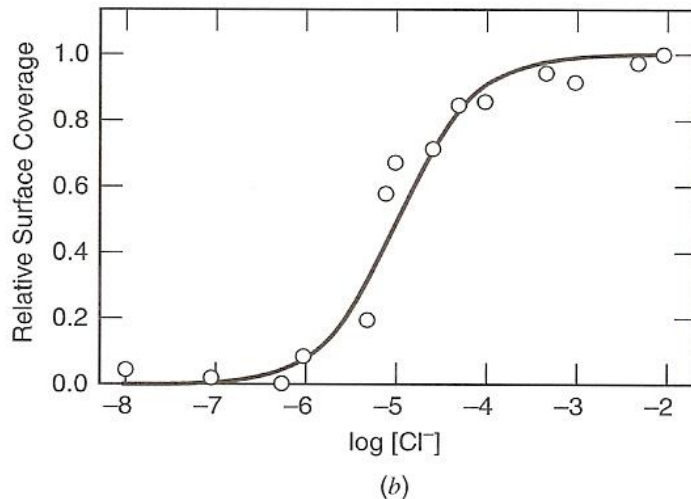
Adsorption isotherm at 0.2 V
    at different KCl
    concentration using
    SHG signal